Electronic Supplementary Information (ESI)

# Multicomponent Polymerization toward Biodegradable Polymers with Diverse Responsiveness in Tumor Microenvironments

*Junnan He, Nan Zheng, Dan Xie, Yubin Zheng *, and Wangze Song **

State Key Laboratory of Fine Chemicals, School of Chemical Engineering, Dalian University of Technology, Linggong Rd.2, Dalian, Liaoning, 116023 (China)

Email: wzsong@dlut.edu.cn (W. Song); zybwl@163.com (Y. Zheng)

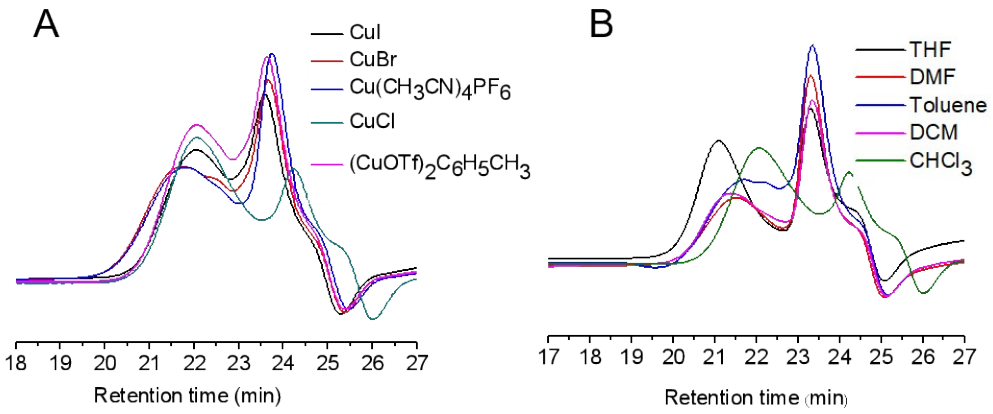


Figure S1. (A) The GPC spectra of polymers (P1) synthesized under different Cu(Ⅰ) catalysts. (B) The GPC spectra of polymers (P1) synthesized under different solvents.

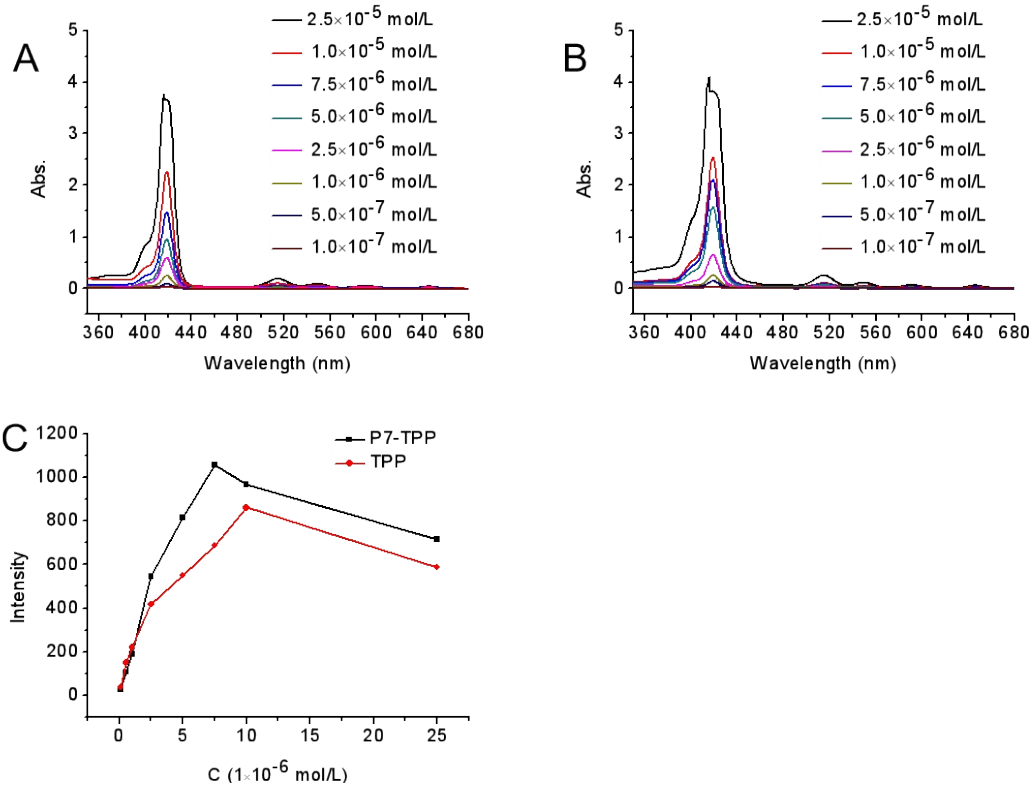


Figure S2. The UV-vis absorption spectra of TPP (A) and P7-TPP (B) at different concentrations. (C) The fluorescence intensities of TPP and P7-TPP at different concentrations (excitation wavelength of 417 nm).

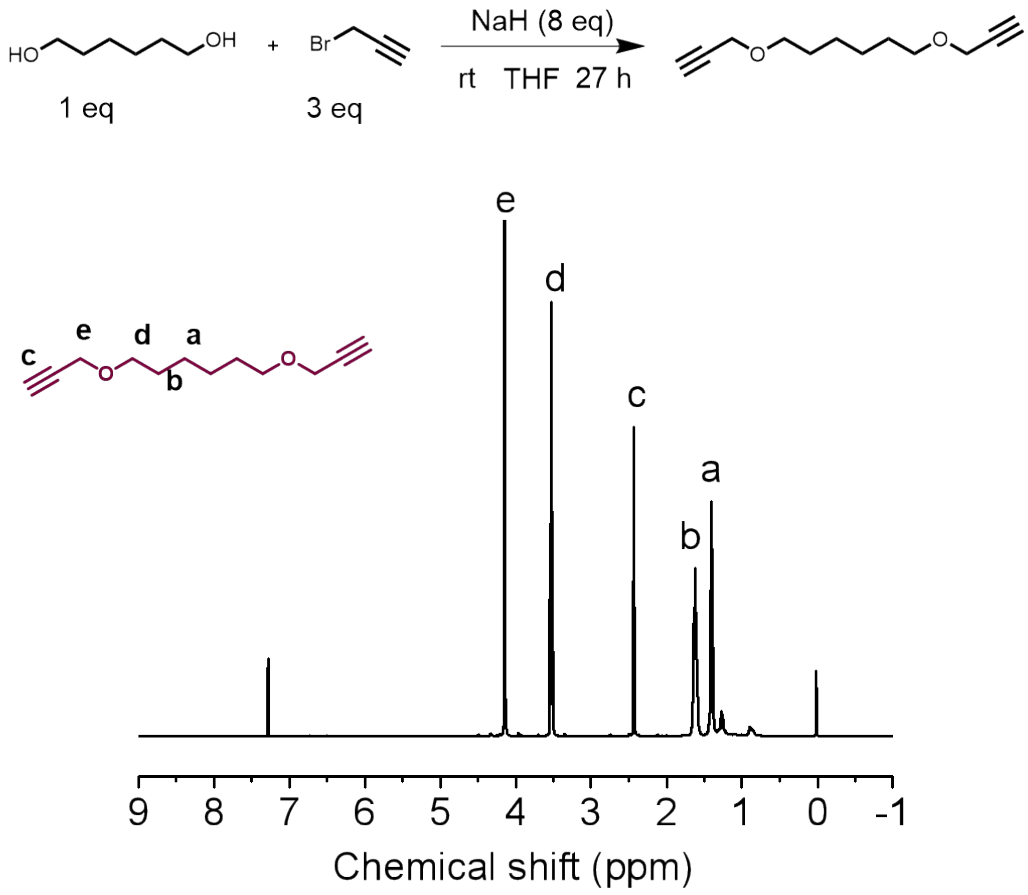


Figure S3. $^{1}H$ NMR spectrum of 1b in $CDCl_3$.

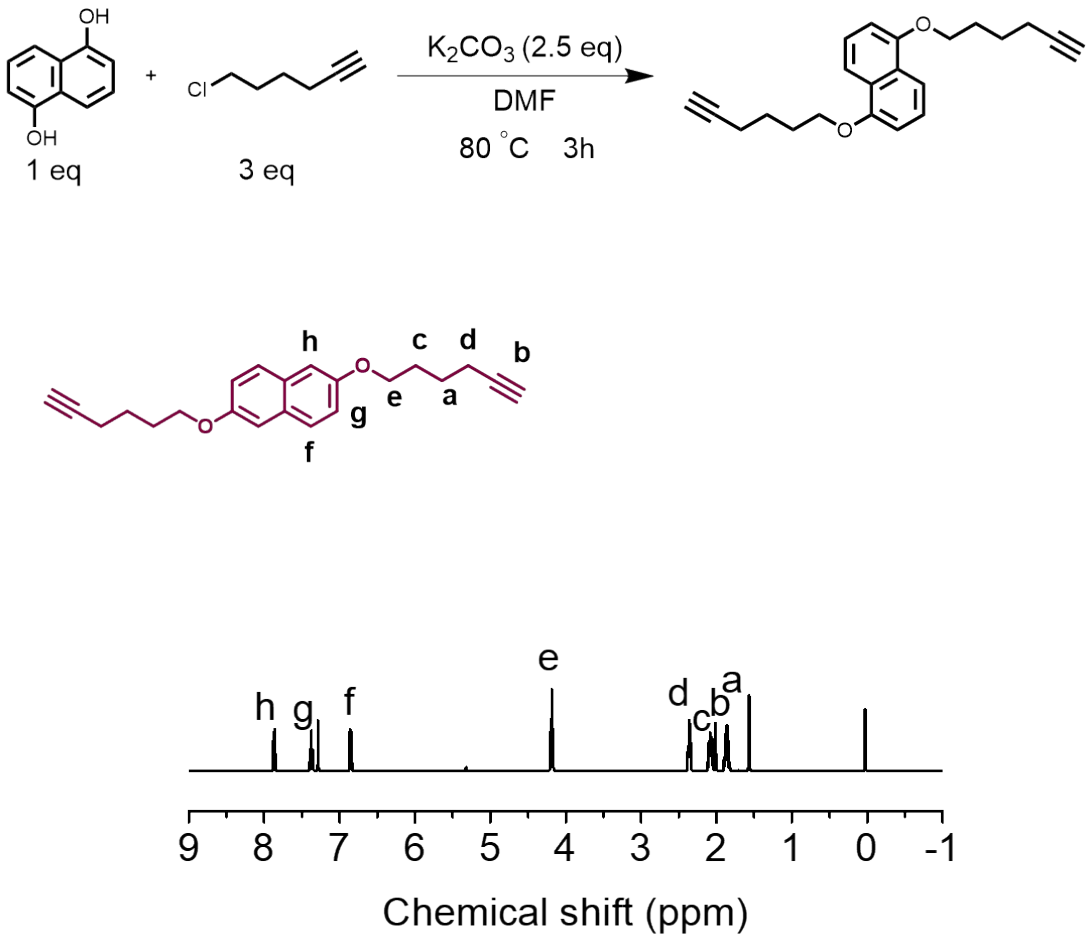


Figure S4. $^{1}H$ NMR spectrum of 1d in $CDCl_3$.

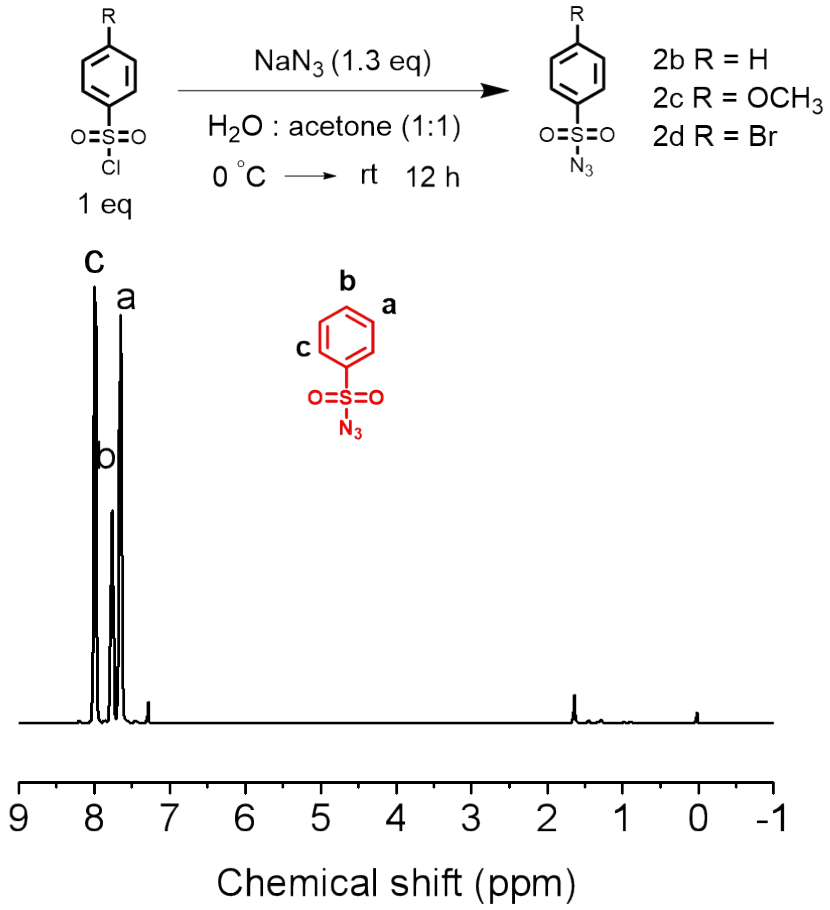


Figure S5. $^{1}H$ NMR spectrum of 2b in $CDCl_3$.

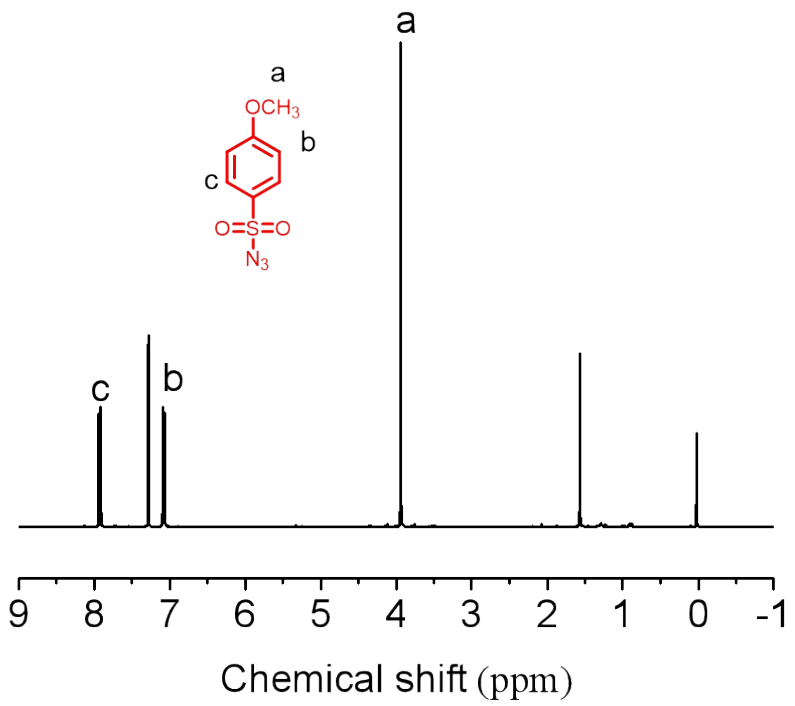


Figure S6. $^{1}H$ NMR spectrum of 2c in $CDCl_3$.

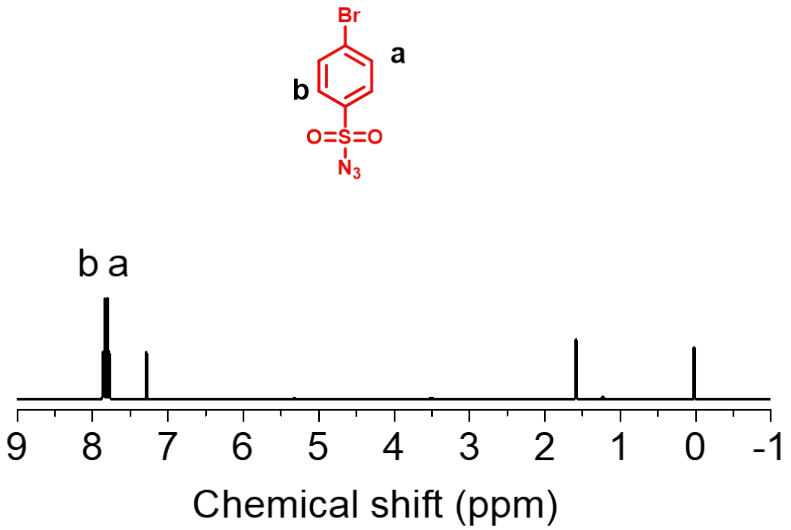


Figure S7. $^{1}H$ NMR spectrum of 2d in $CDCl_3$.

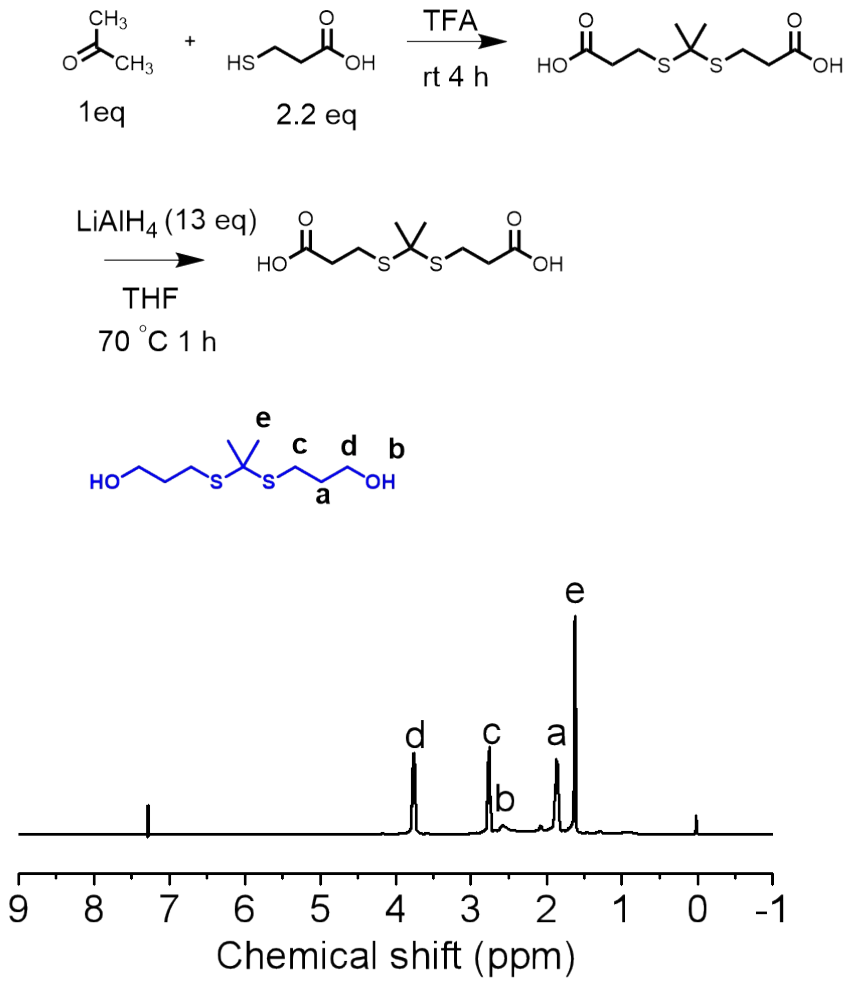


Figure S8. $^{1}H$ NMR spectrum of 3a in $CDCl_3$.

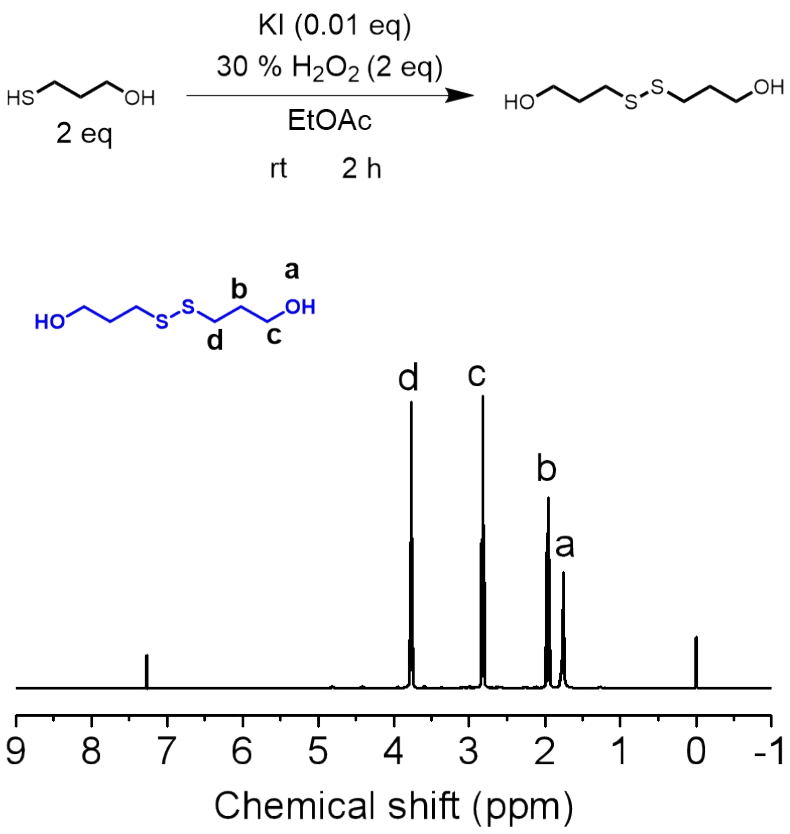


Figure S9. $^{1}$H NMR spectrum of 3b in *d*-DMSO.

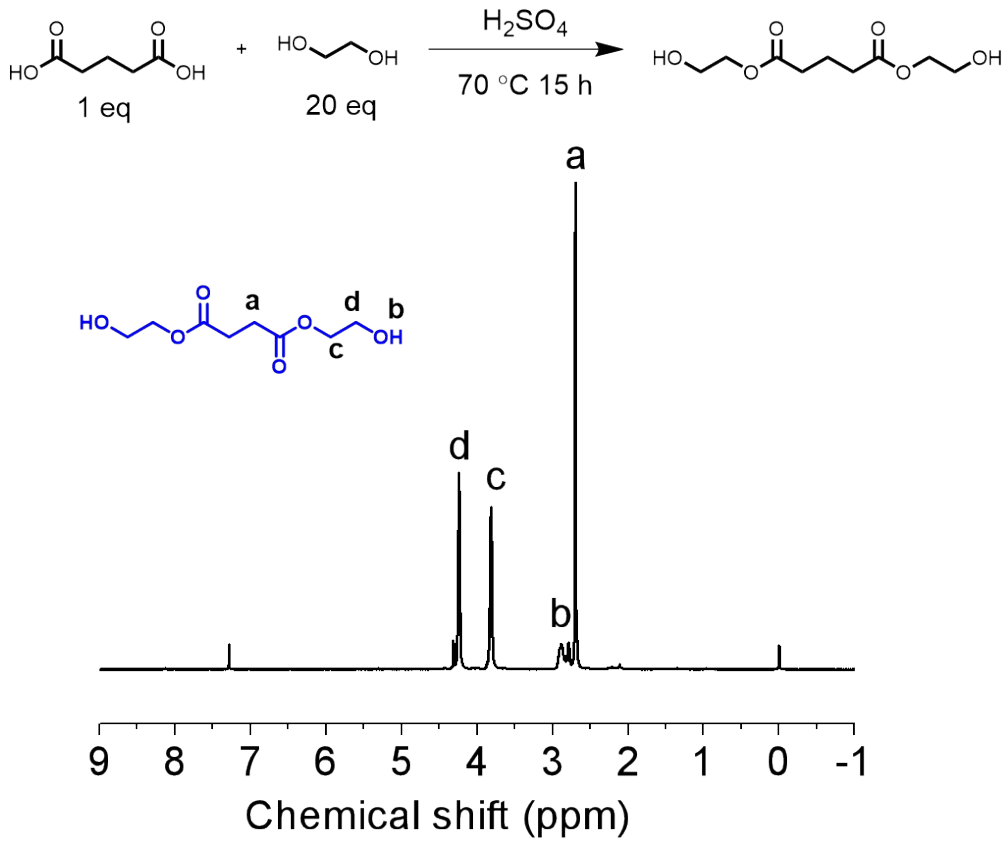


Figure S10. $^{1}H$ NMR spectrum of 3c in $CDCl_3$.

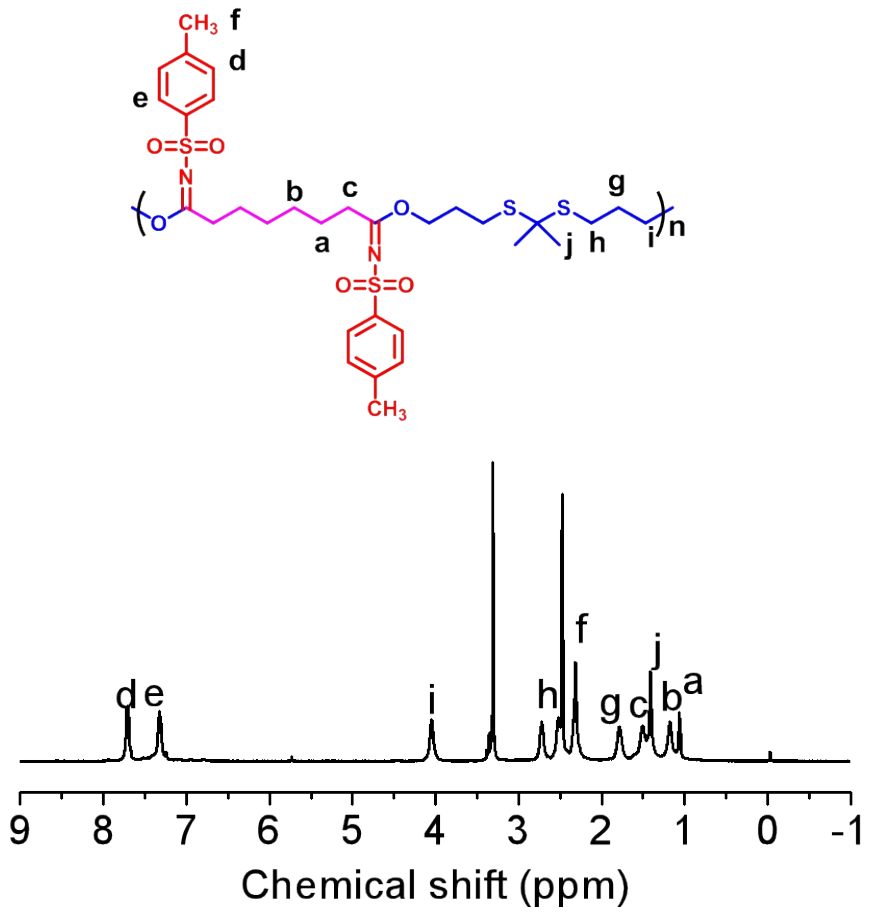


Figure S11. $^{1}$H NMR spectrum of P1 (P1a/2a/3a) in *d*-DMSO.

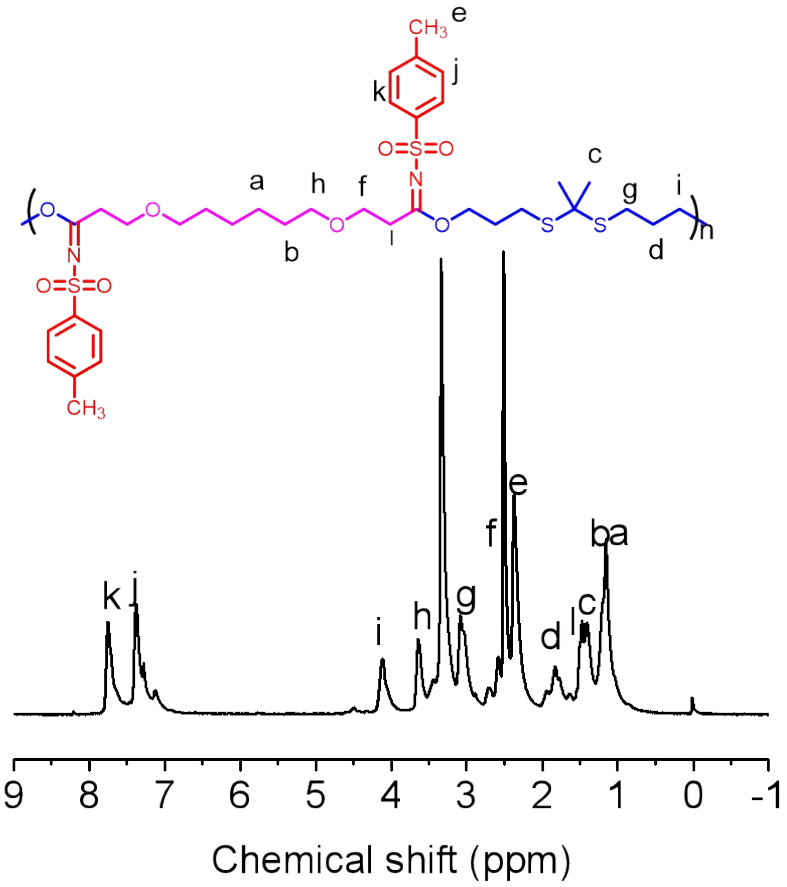


Figure S12. $^{1}$H NMR spectrum of P2 (P1b/2a/3a) in *d*-DMSO.

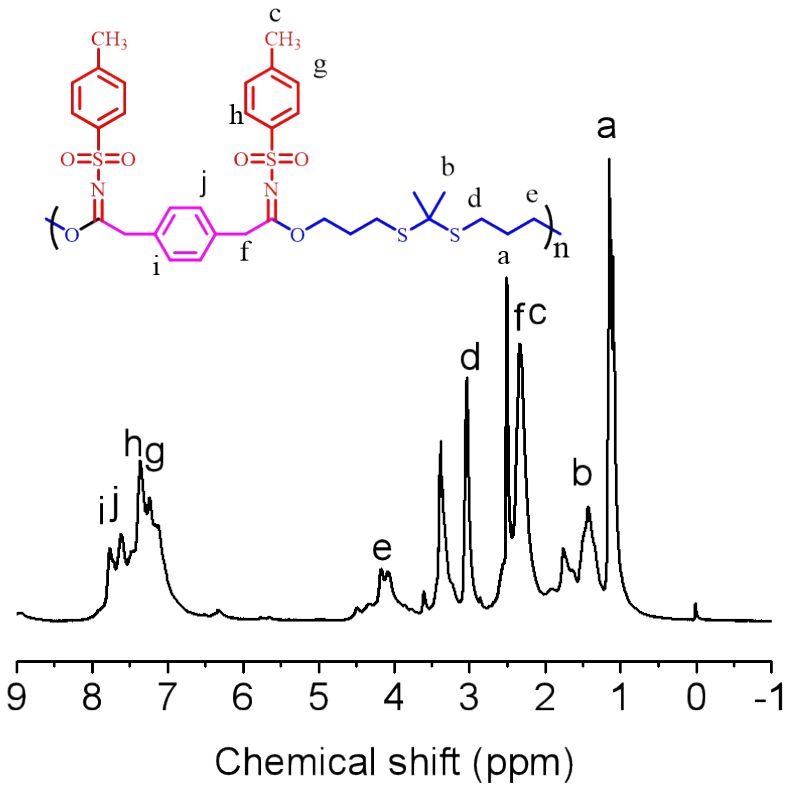


Figure S13. $^{1}$H NMR spectrum of P3 (P1c/2a/3a) in *d*-DMSO.

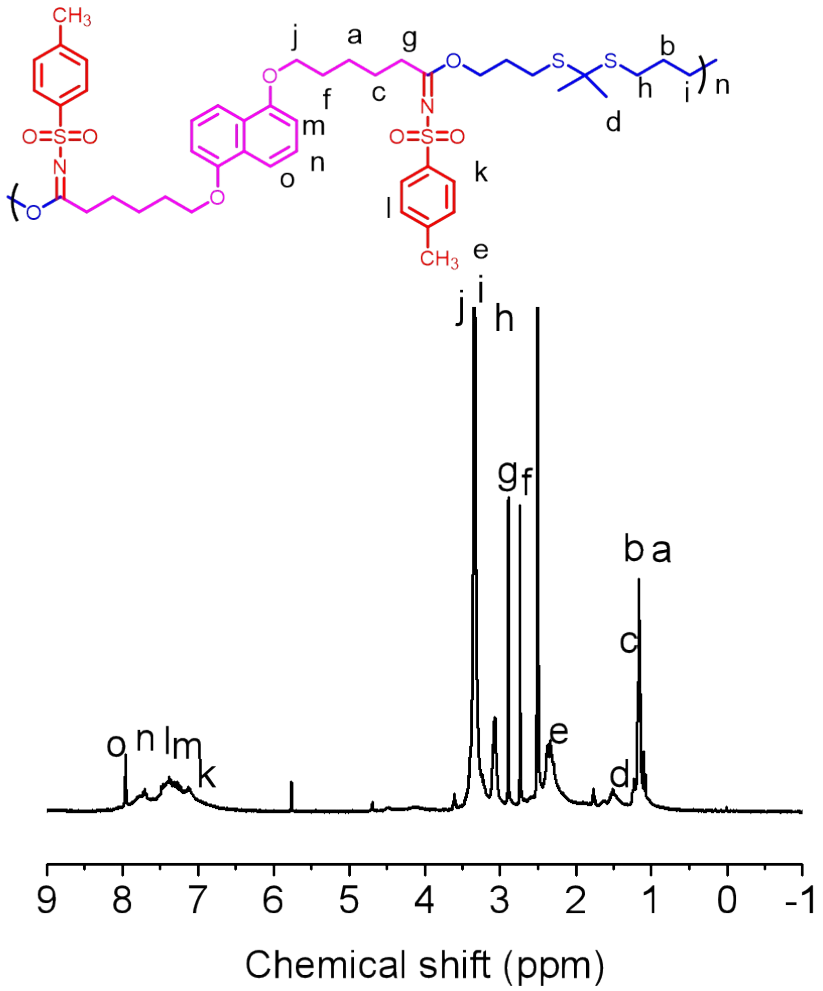


Figure S14. $^{1}$H NMR spectrum of P4 (P1d/2a/3a) in *d*-DMSO.

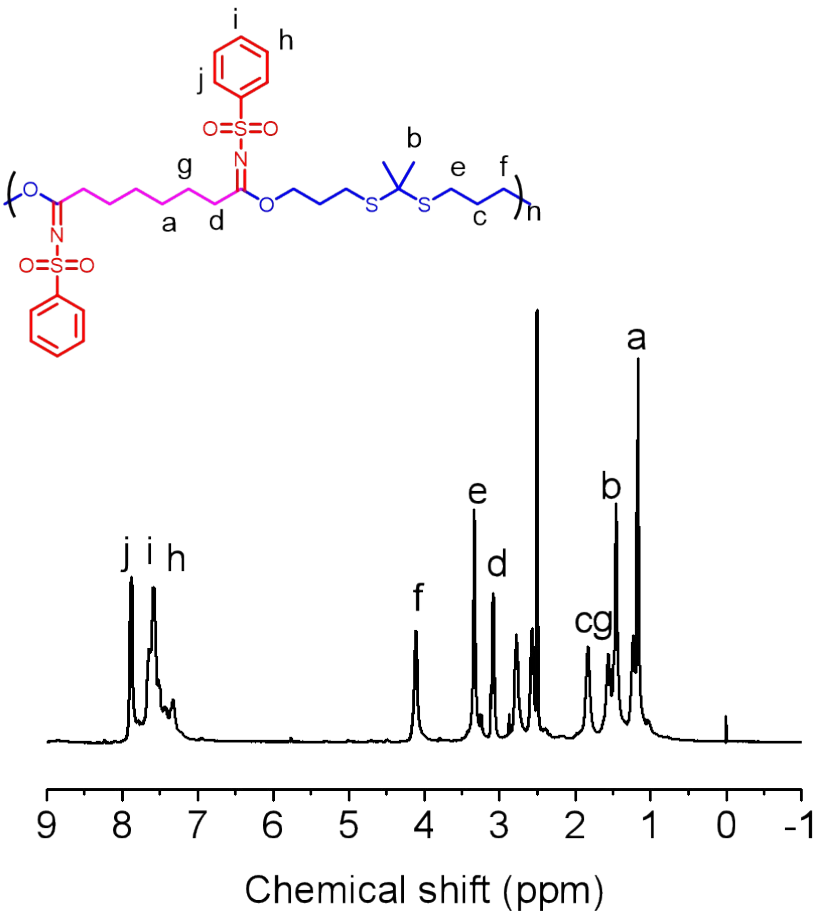


Figure S15. $^{1}$H NMR spectrum of P5 (P1a/2b/3a) in *d*-DMSO.

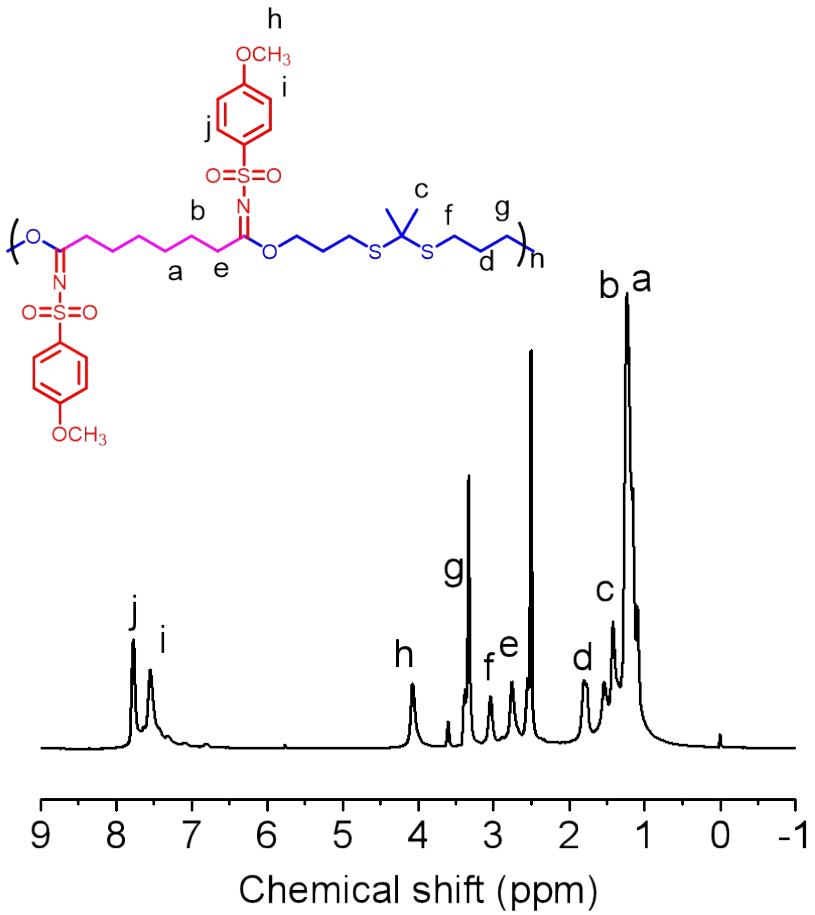


Figure S16. $^{1}$H NMR spectrum of P6 (P1a/2c/3a) in *d*-DMSO.

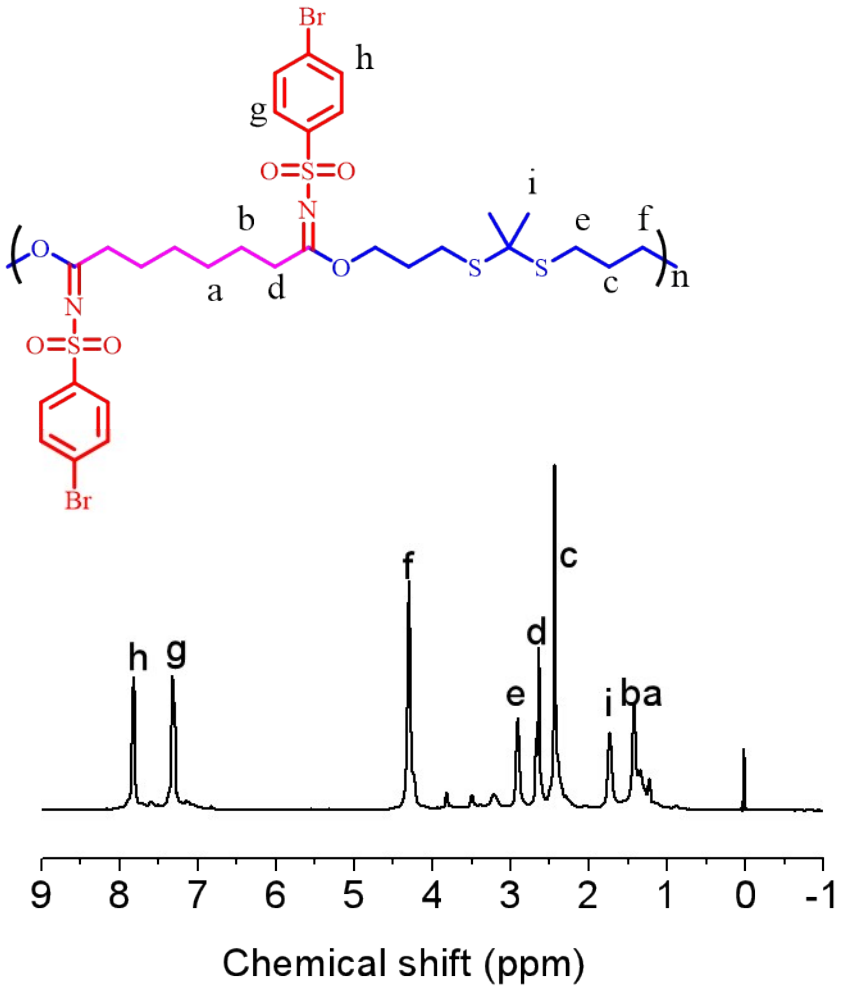


Figure S17. $^{1}$H NMR spectrum of P7 (P1a/2d/3a) in *d*-DMSO.

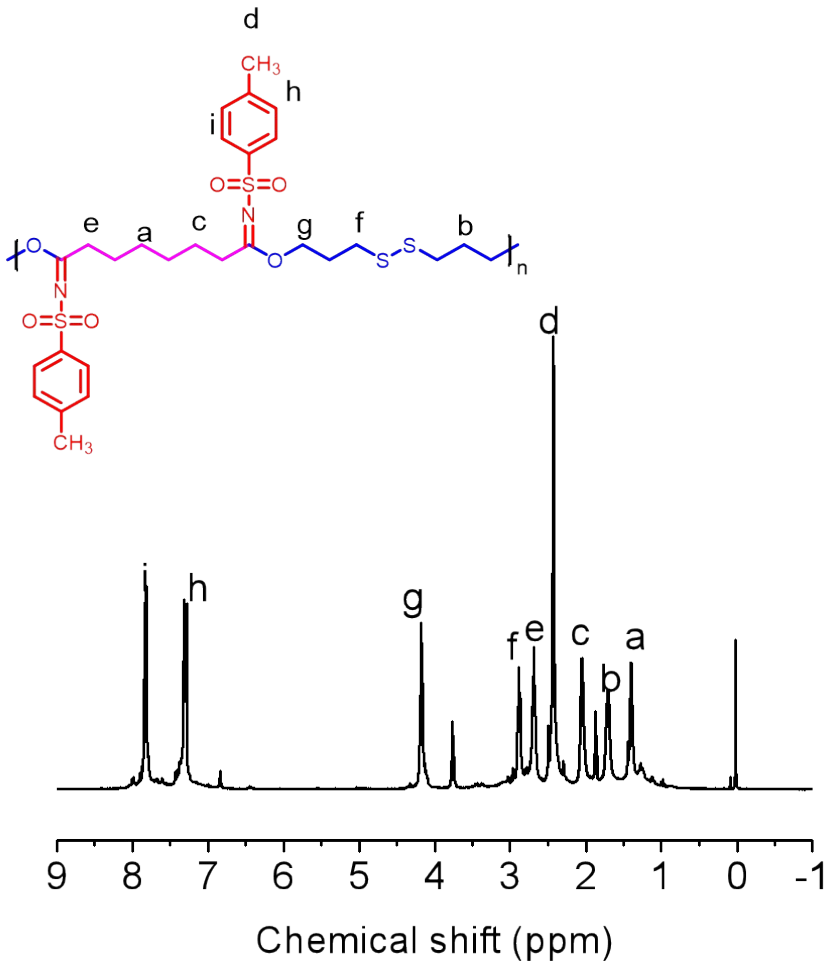


Figure S18. $^{1}$H NMR spectrum of P8 (P1a/2a/3b) in *d*-DMSO.

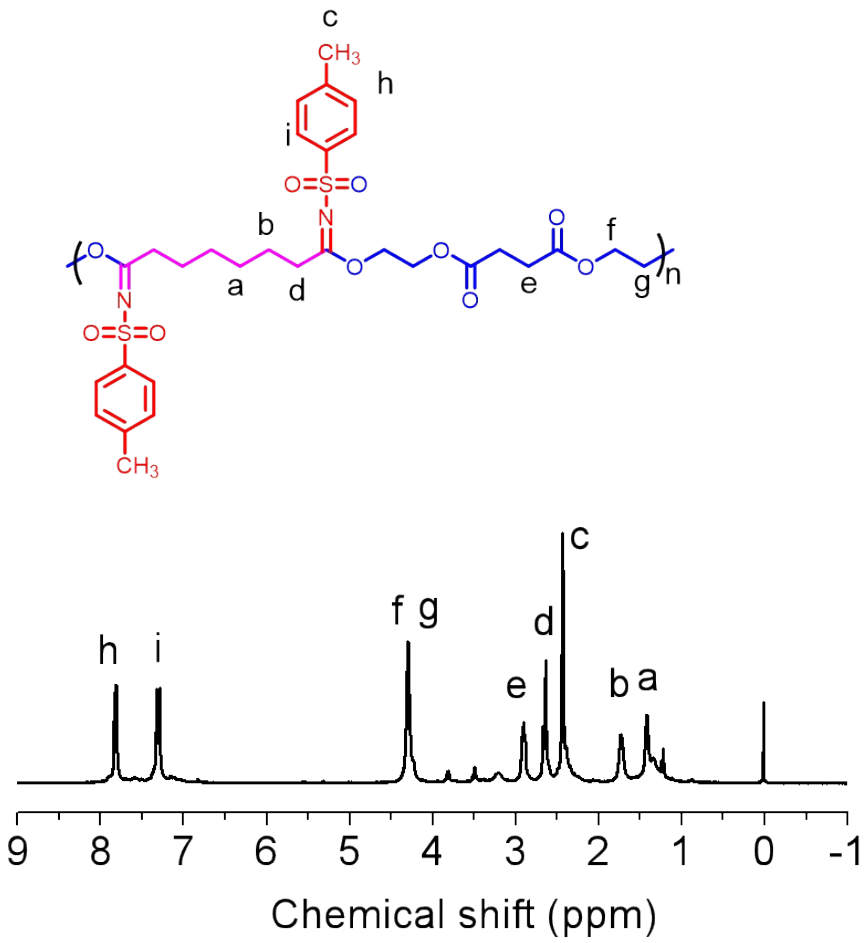


Figure S19. $^{1}$H NMR spectrum of P9 (P1a/2a/3c) in *d*-DMSO.

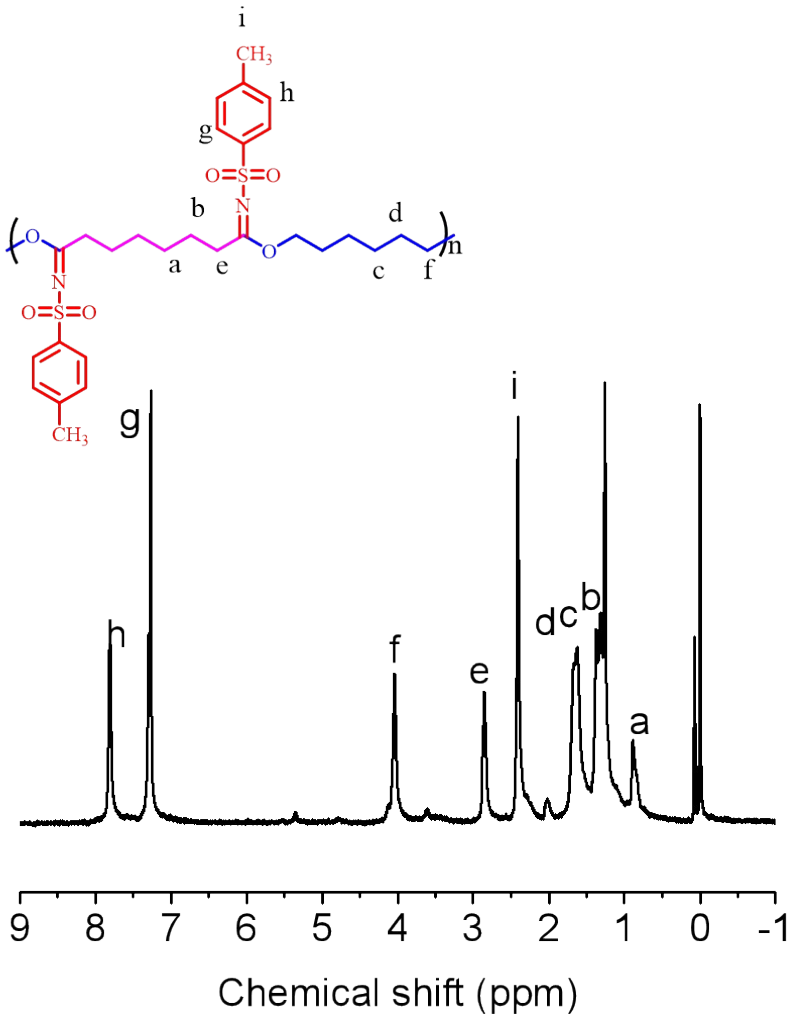


Figure S20. $^{1}$H NMR spectrum of P10 (P1a/2a/3d) in *d*-DMSO.

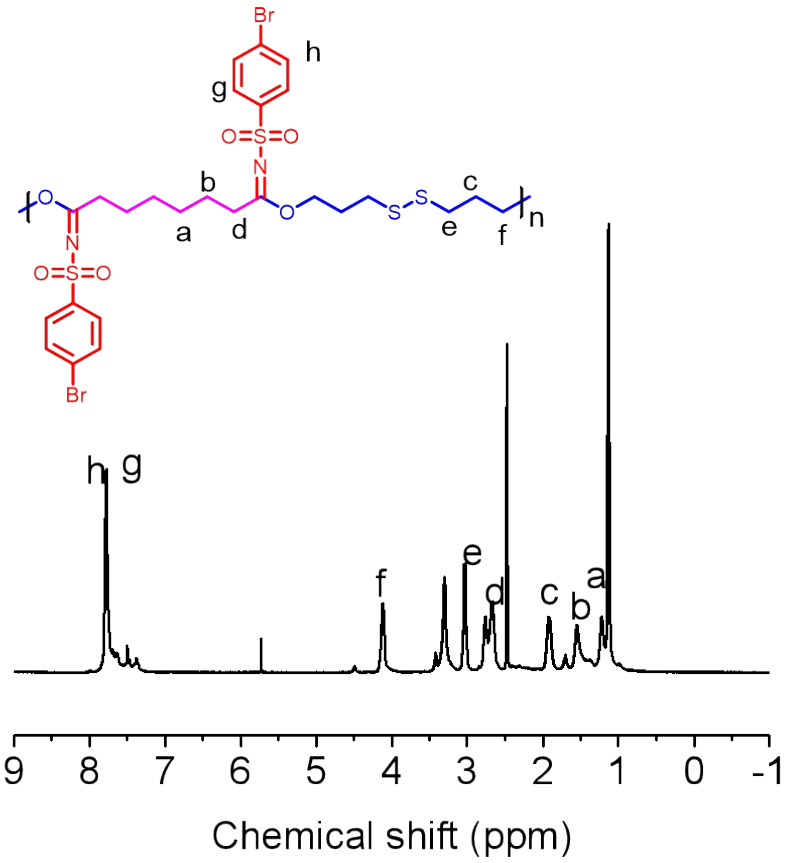


Figure S21. $^{1}H$ NMR spectrum of P11 (P1a/2d/3b) in *d*-DMSO.

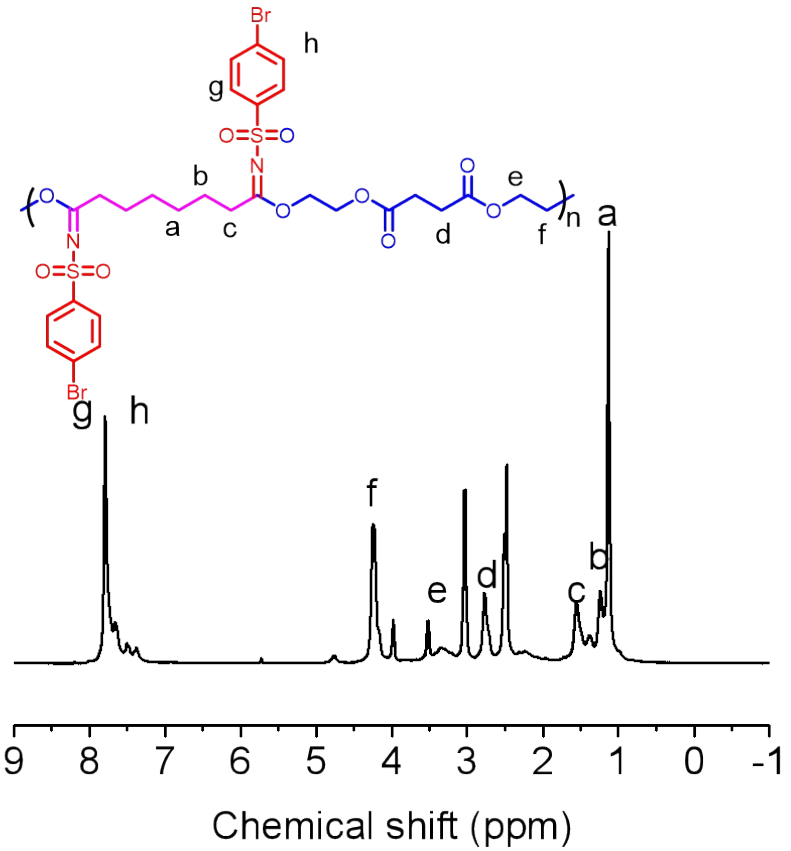


Figure S22. $^{1}$H NMR spectrum of P12 (P1a/2d/3c) in *d*-DMSO.

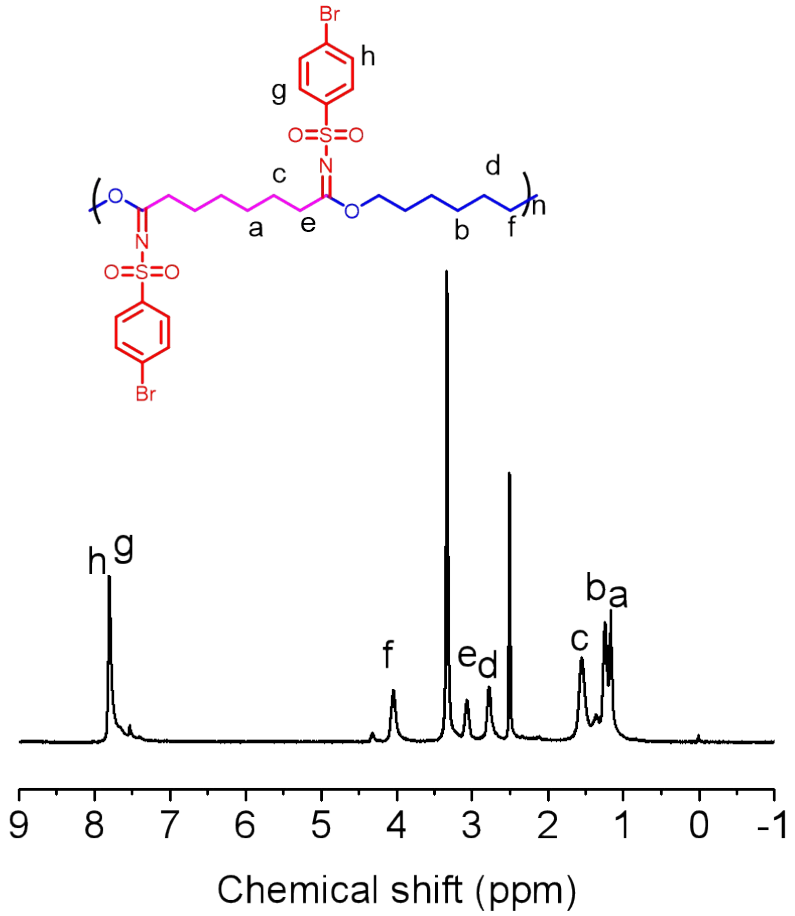


Figure S23. $^{1}$H NMR spectrum of P13 (P1a/2d/3d) in *d*-DMSO.

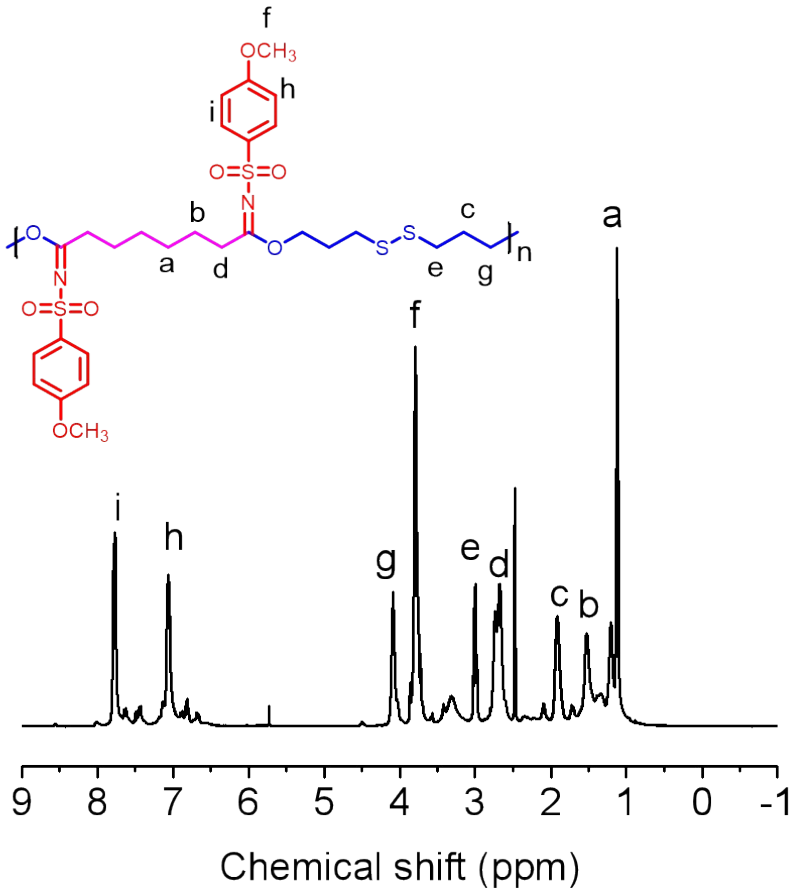


Figure S24. $^{1}$H NMR spectrum of P14 (P1a/2c/3b) in *d*-DMSO.

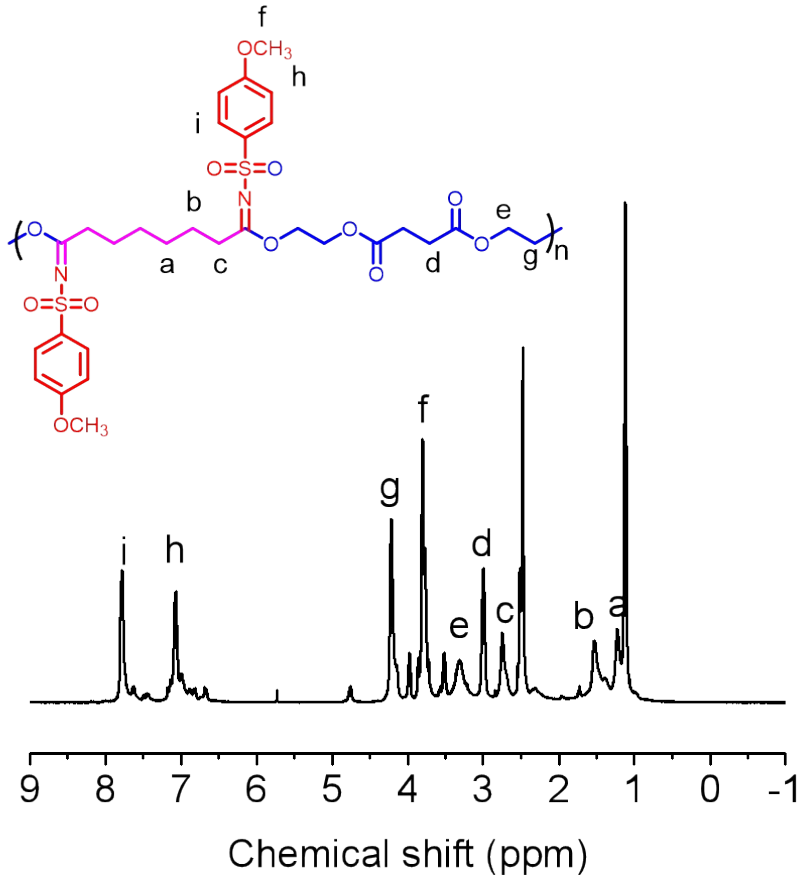


Figure S25. $^{1}$H NMR spectrum of P15 (P1a/2c/3c) in *d*-DMSO.

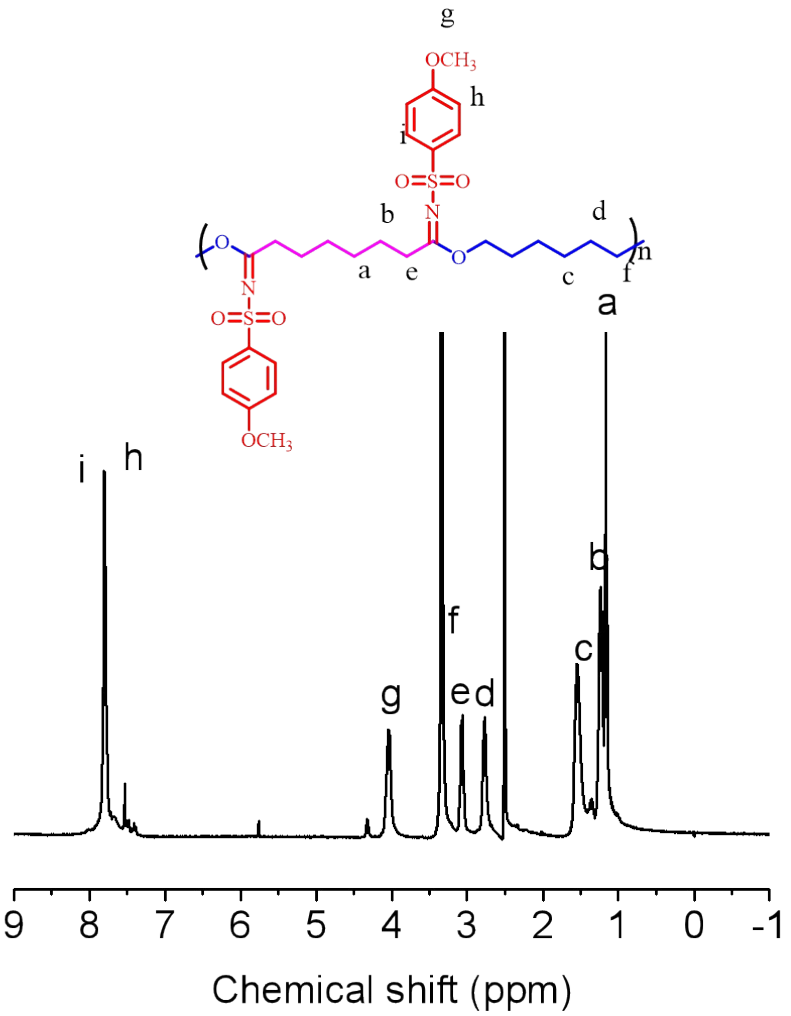


Figure S26. $^{1}$H NMR spectrum of P16 (P1a/2c/3d) in *d*-DMSO.

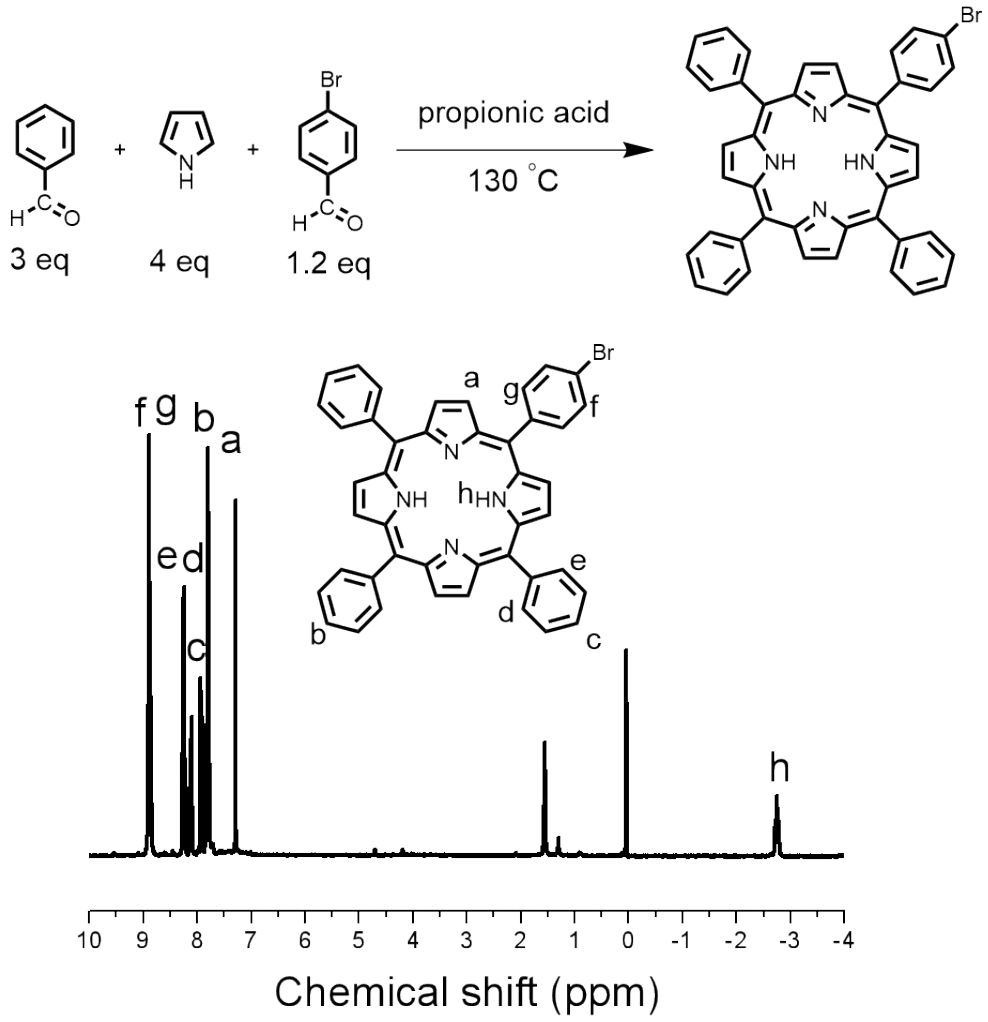


Figure S27. $^{1}H$ NMR spectrum of TPP-Br in $CDCl_3$.

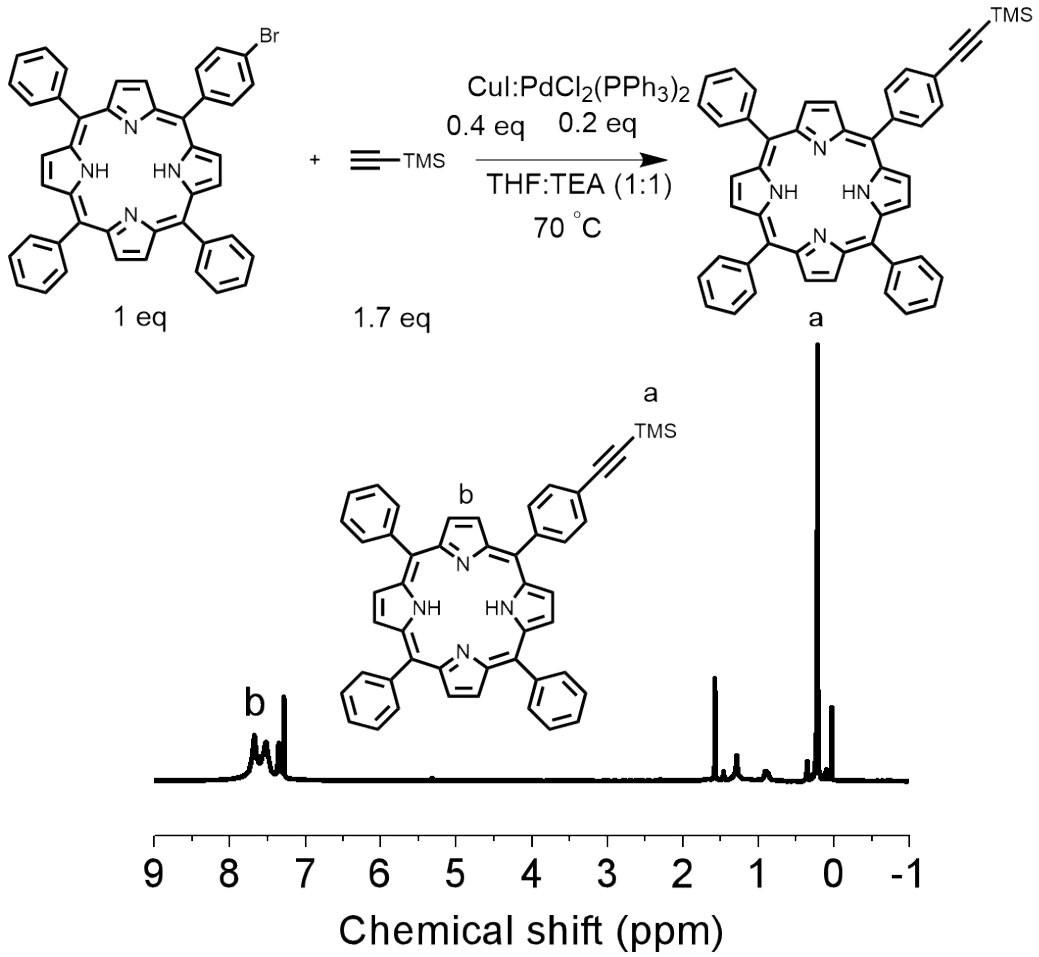


Figure S28. $^{1}H$ NMR spectrum of TPP-yne-TMS in $CDCl_3$.

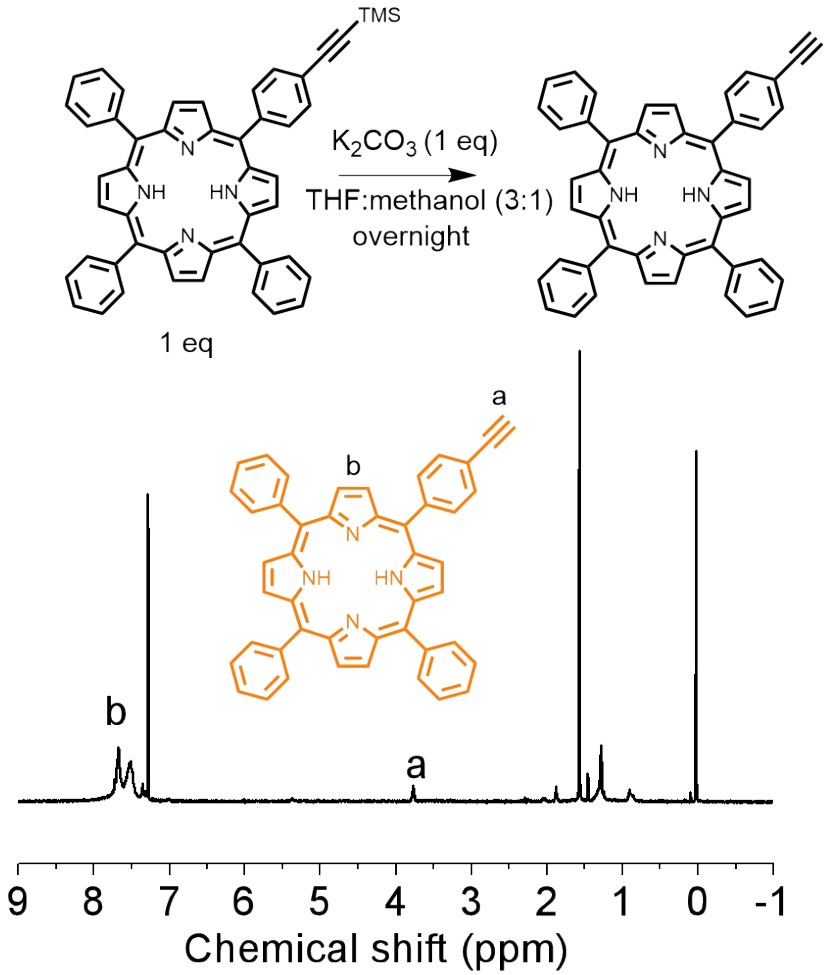


Figure S29. $^{1}H$ NMR spectrum of TPP-yne in $CDCl_3$.

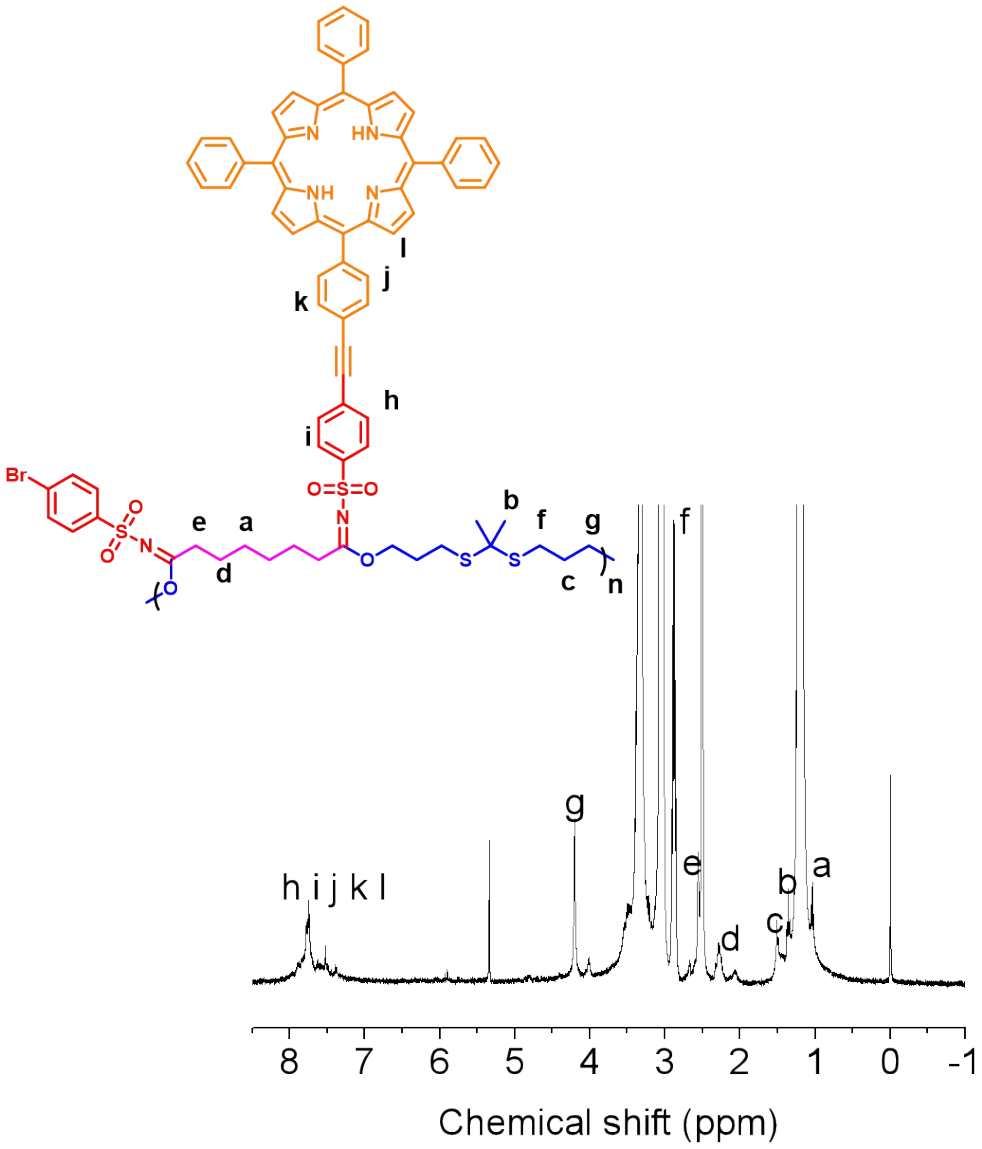


Figure S30. $^{1}$H NMR spectrum of P7-TPP synthesized by one-pot, four-component, tandem polymerization in *d*-DMSO.

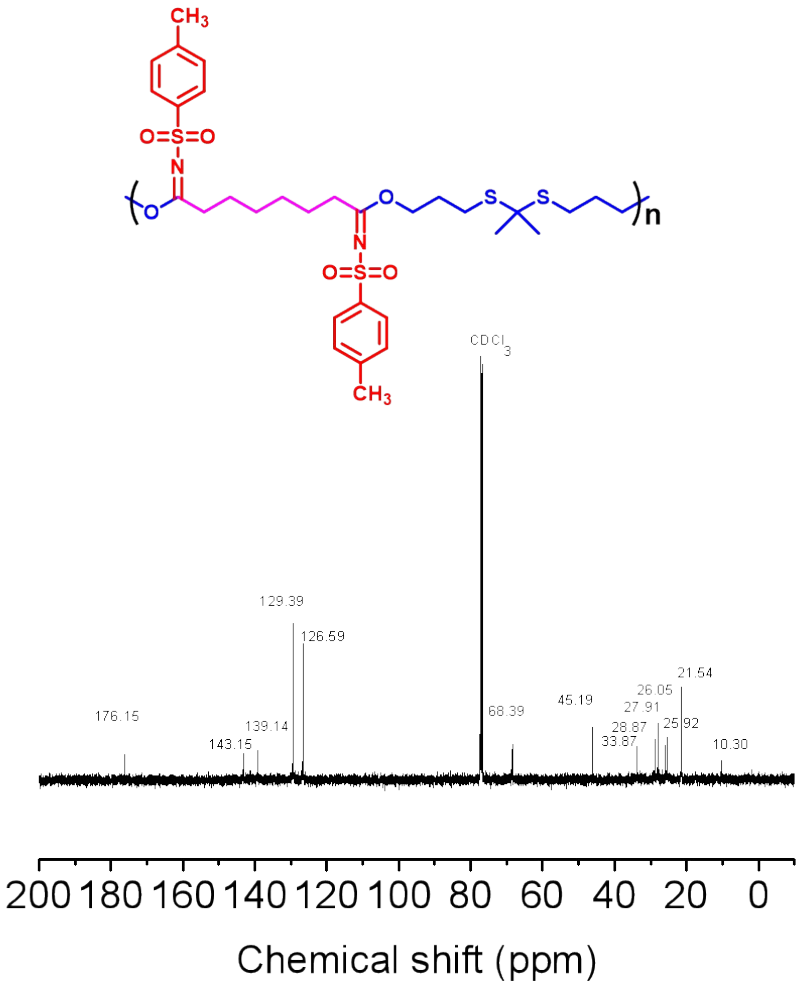


Figure S31. $^{13}C$ NMR spectrum of P1 (P1a/2a/3a) in $CDCl_3$.

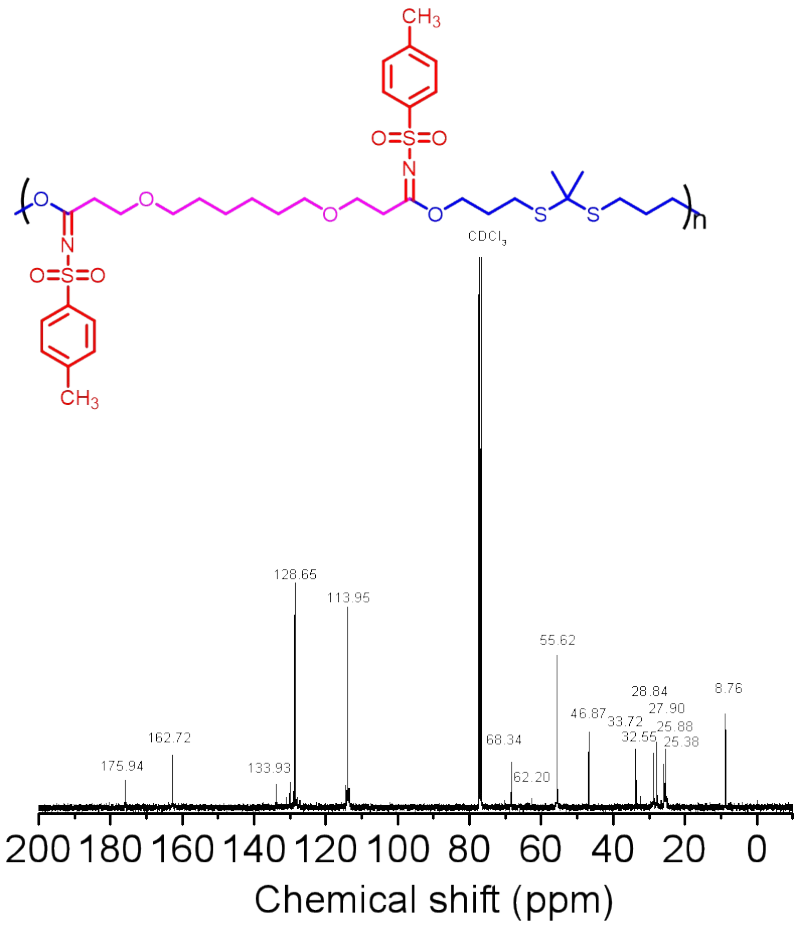


Figure S32. $^{13}C$ NMR spectrum of P2 (P1b/2a/3a) in $CDCl_3$.

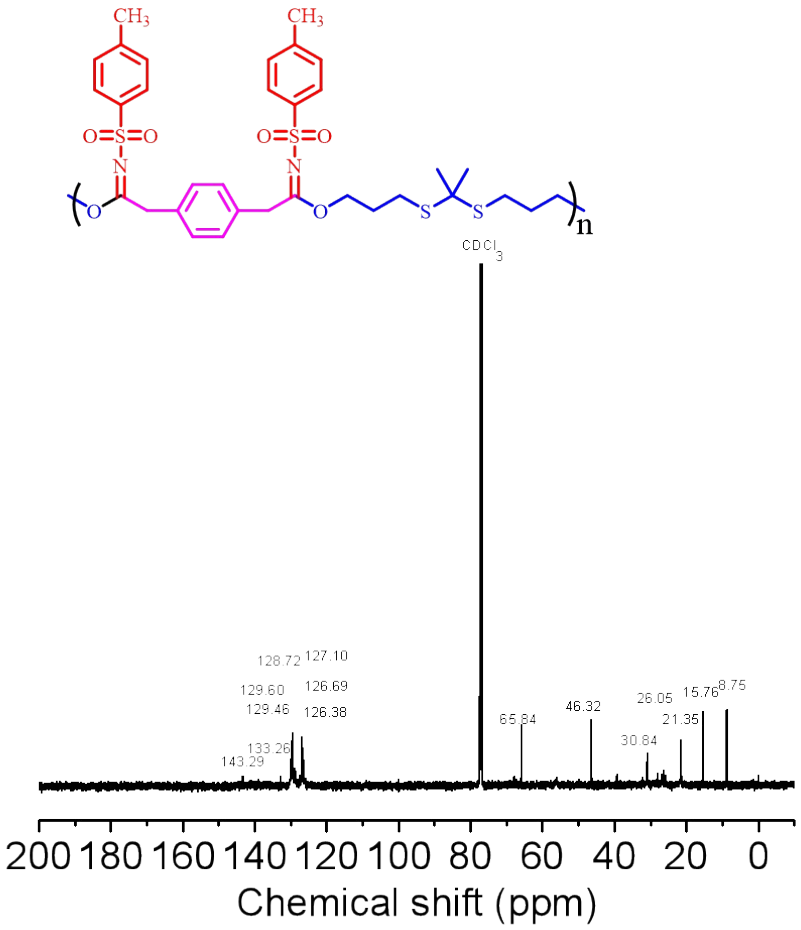


Figure S33. $^{13}C$ NMR spectrum of P3 (P1c/2a/3a) in $CDCl_3$.

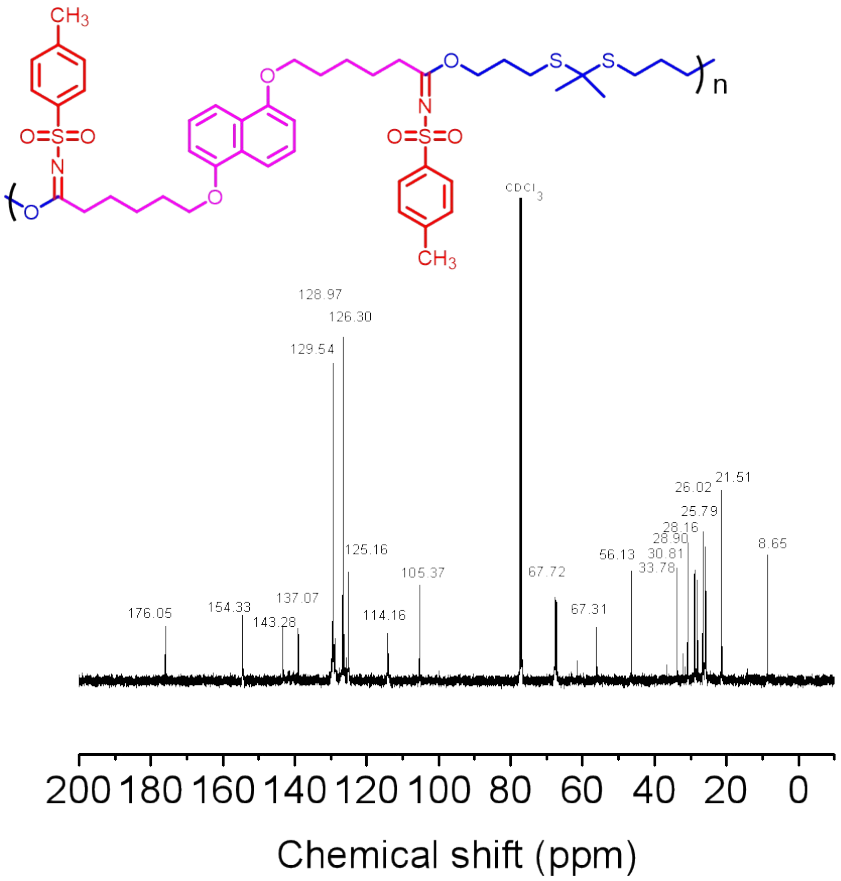


Figure S34. $^{13}C$ NMR spectrum of P4 (P1d/2a/3a) in $CDCl_3$.

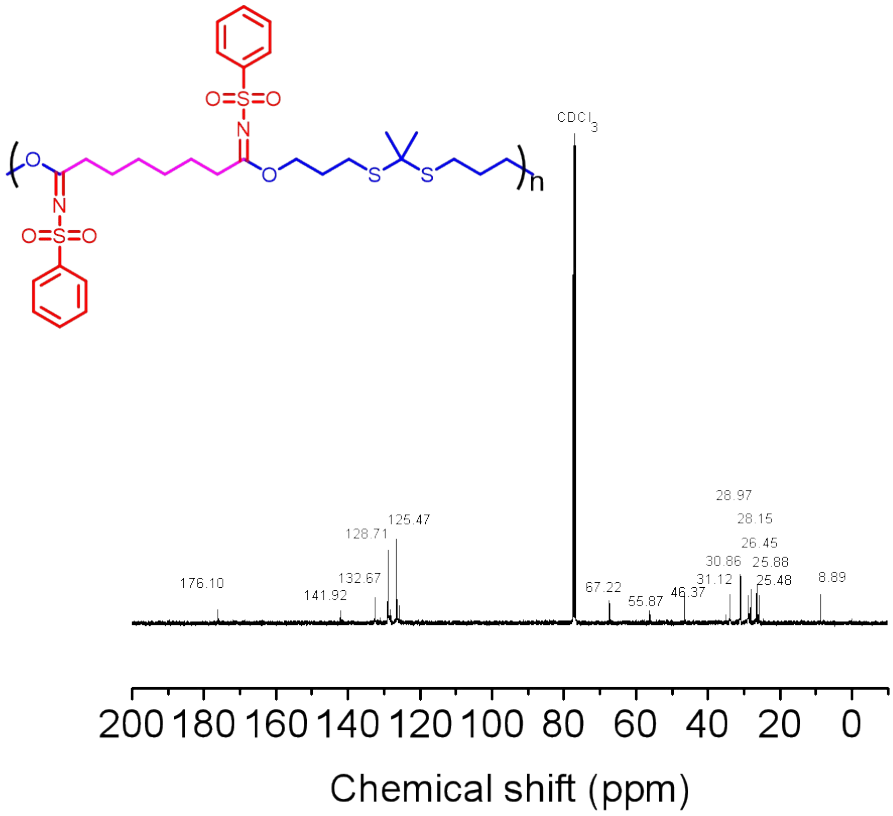


Figure S35. $^{13}C$ NMR spectrum of P5 (P1a/2b/3a) in $CDCl_3$.

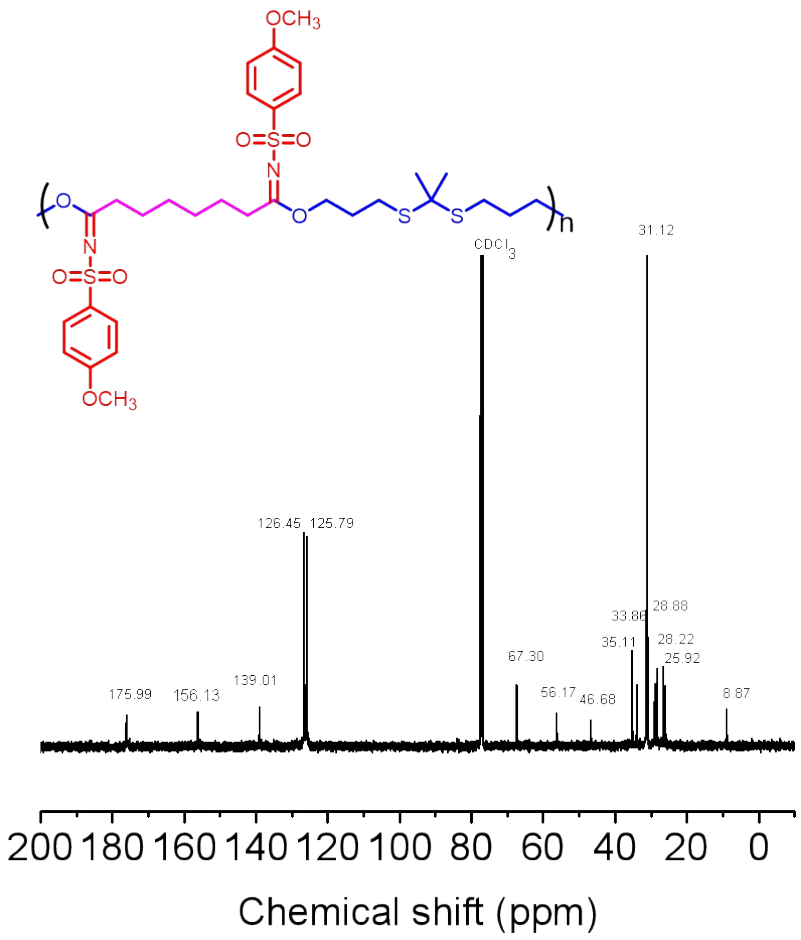


Figure S36. $^{13}C$ NMR spectrum of P6 (P1a/2c/3a) in $CDCl_3$.

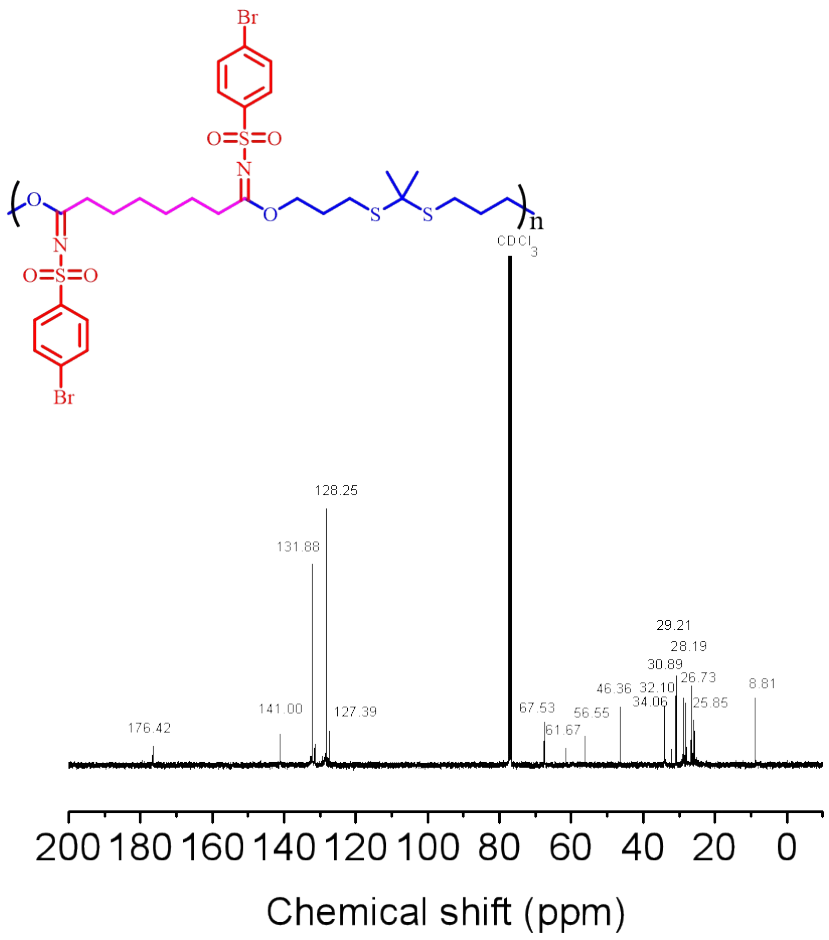


Figure S37. $^{13}C$ NMR spectrum of P7 (P1a/2d/3a) in $CDCl_3$.

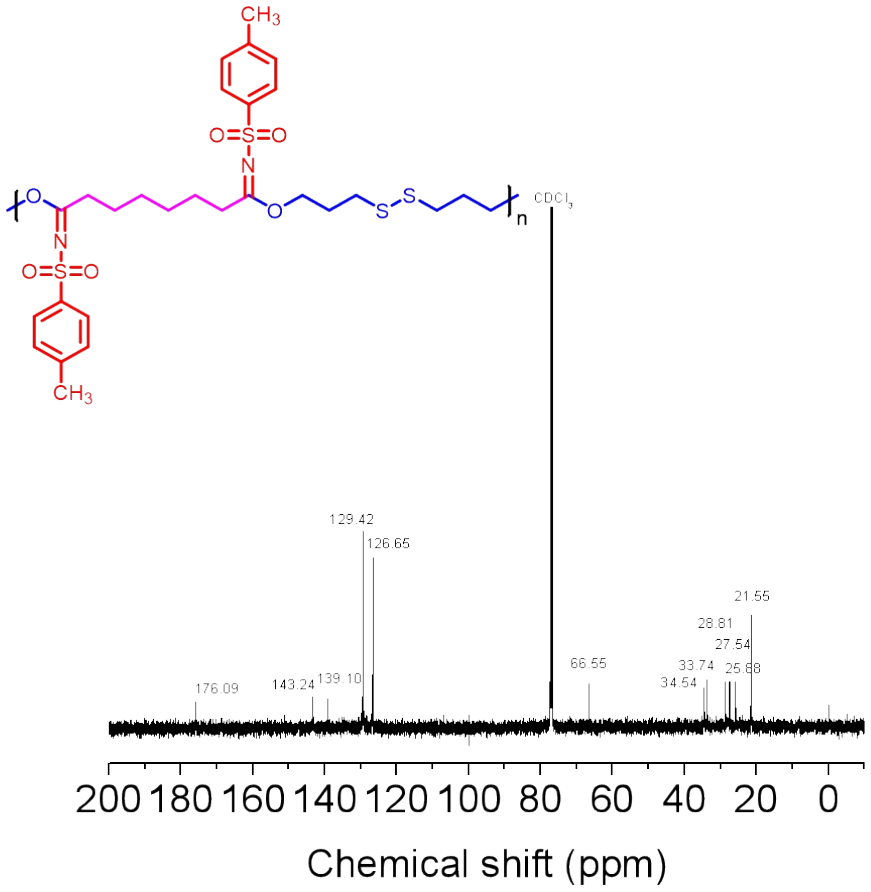


Figure S38. $^{13}C$ NMR spectrum of P8 (P1a/2a/3b) in $CDCl_3$.

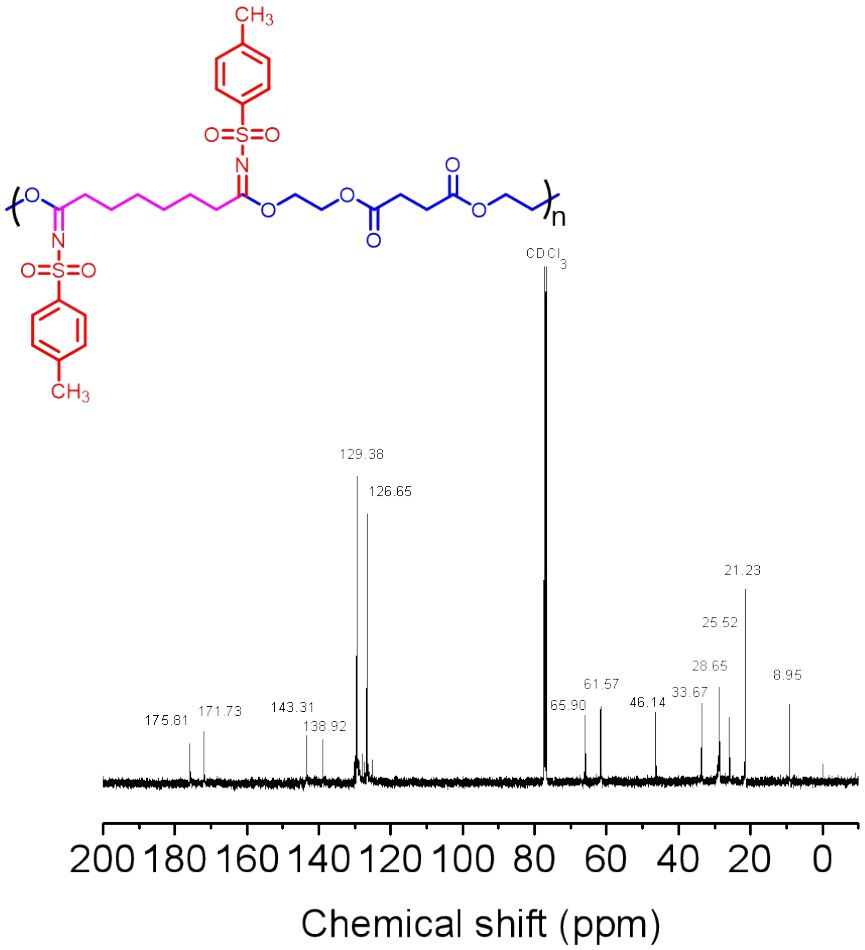


Figure S39. $^{13}C$ NMR spectrum of P9 (P1a/2a/3c) in $CDCl_3$.

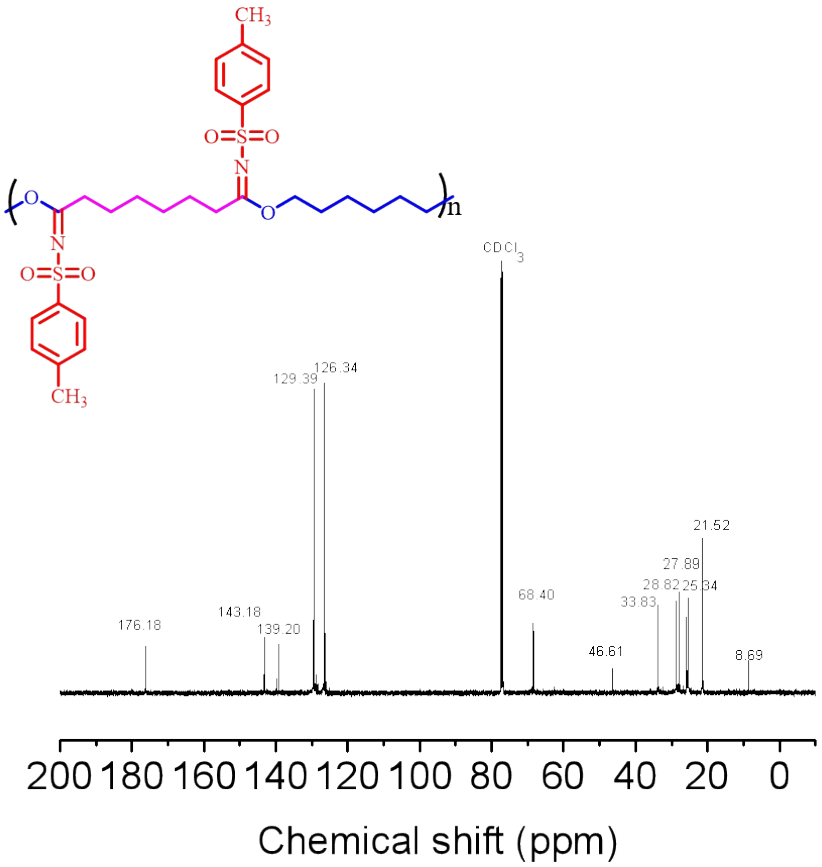


Figure S40. $^{13}C$ NMR spectrum of P10 (P1a/2a/3d) in $CDCl_3$.

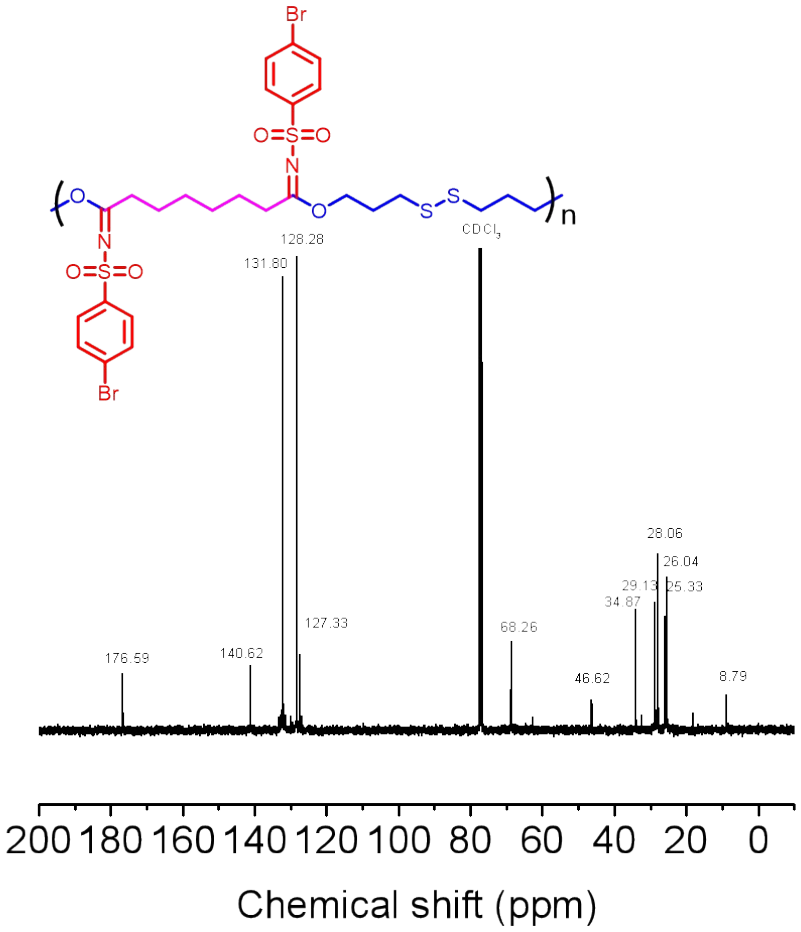


Figure S41. $^{13}C$ NMR spectrum of P11 (P1a/2d/3b) in $CDCl_3$.

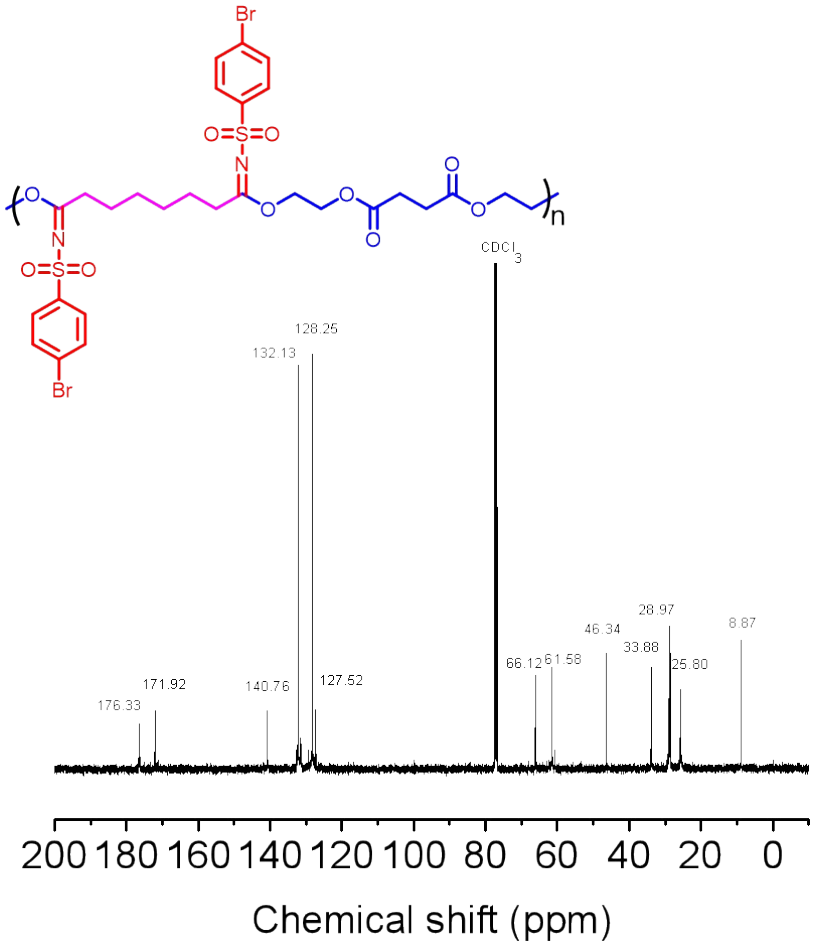


Figure S42. $^{13}C$ NMR spectrum of P12 (P1a/2d/3c) in $CDCl_3$.

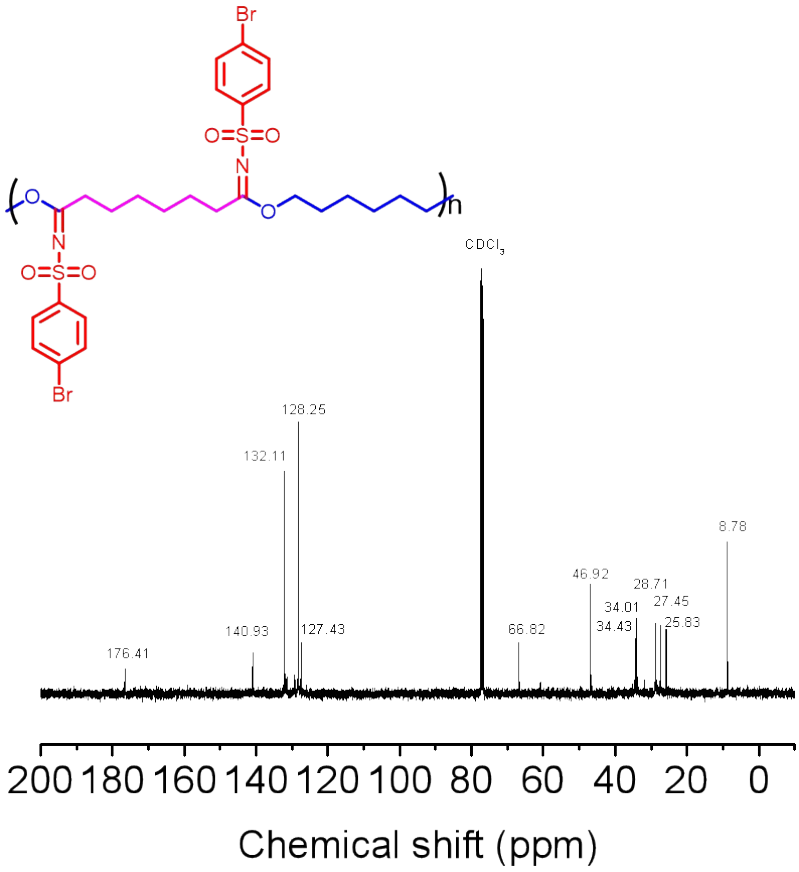


Figure S43. $^{13}C$ NMR spectrum of P13 (P1a/2d/3d) in $CDCl_3$.

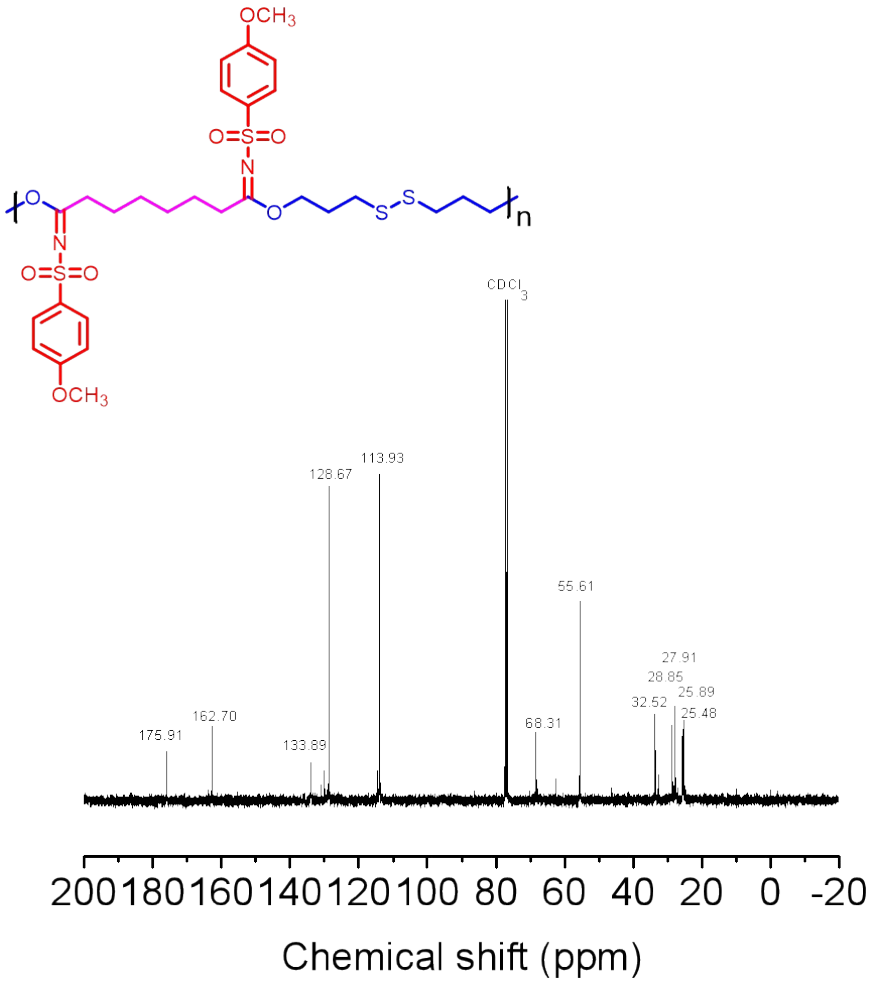


Figure S44. $^{13}C$ NMR spectrum of P14 (P1a/2c/3b) in $CDCl_3$.

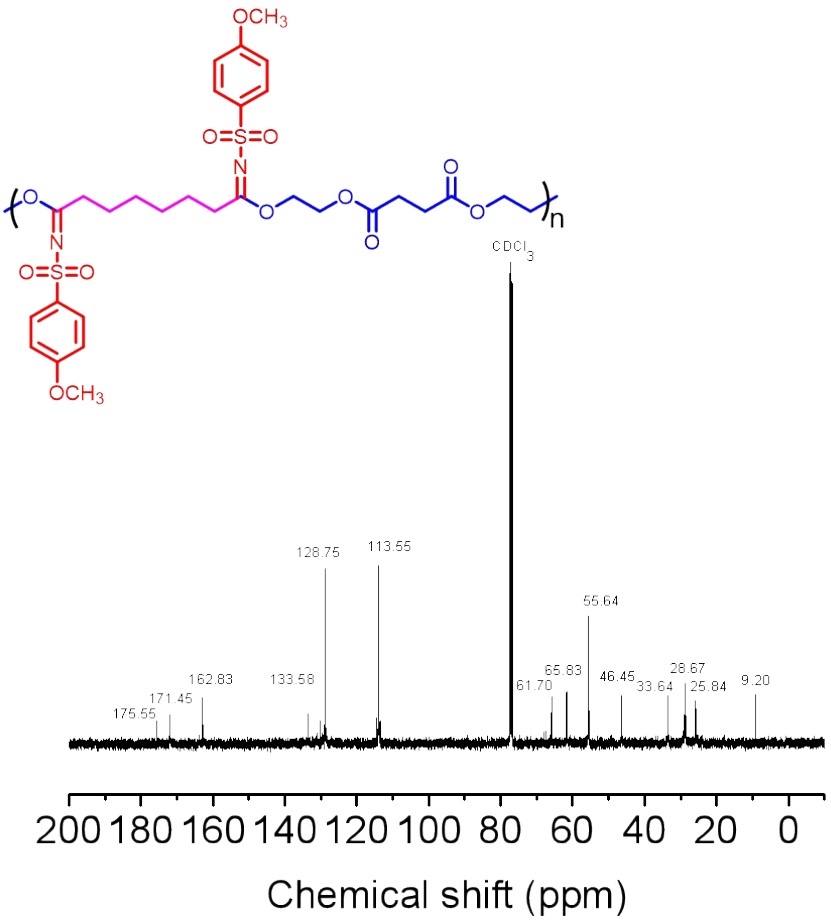


Figure S45. $^{13}C$ NMR spectrum of P15 (P1a/2c/3c) in $CDCl_3$.

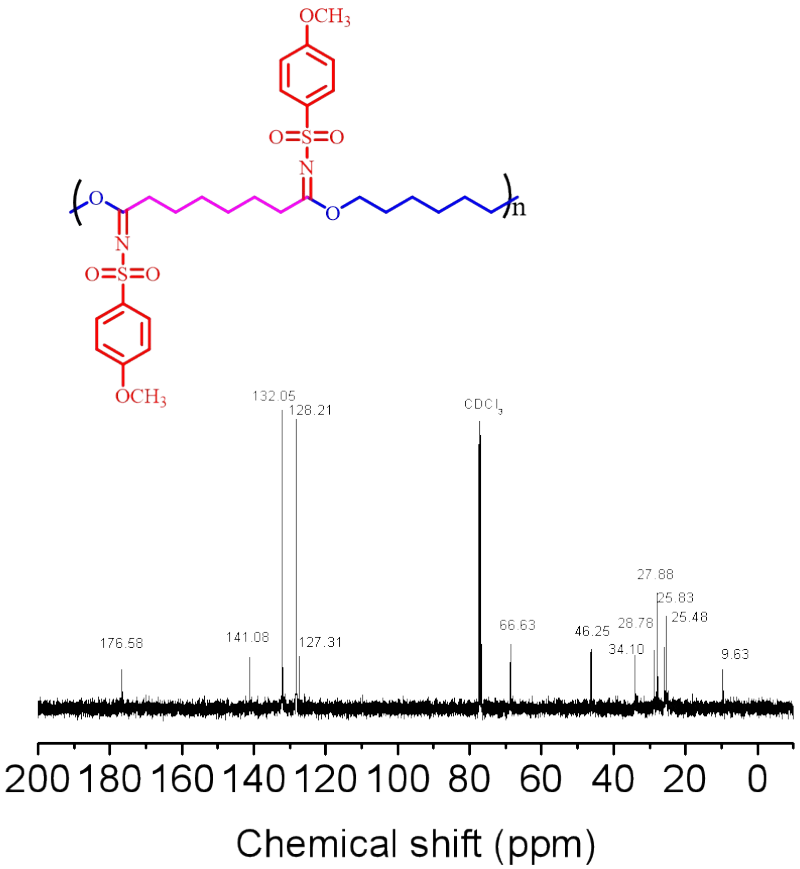


Figure S46. $^{13}C$ NMR spectrum of P16 (P1a/2c/3d) in $CDCl_3$.

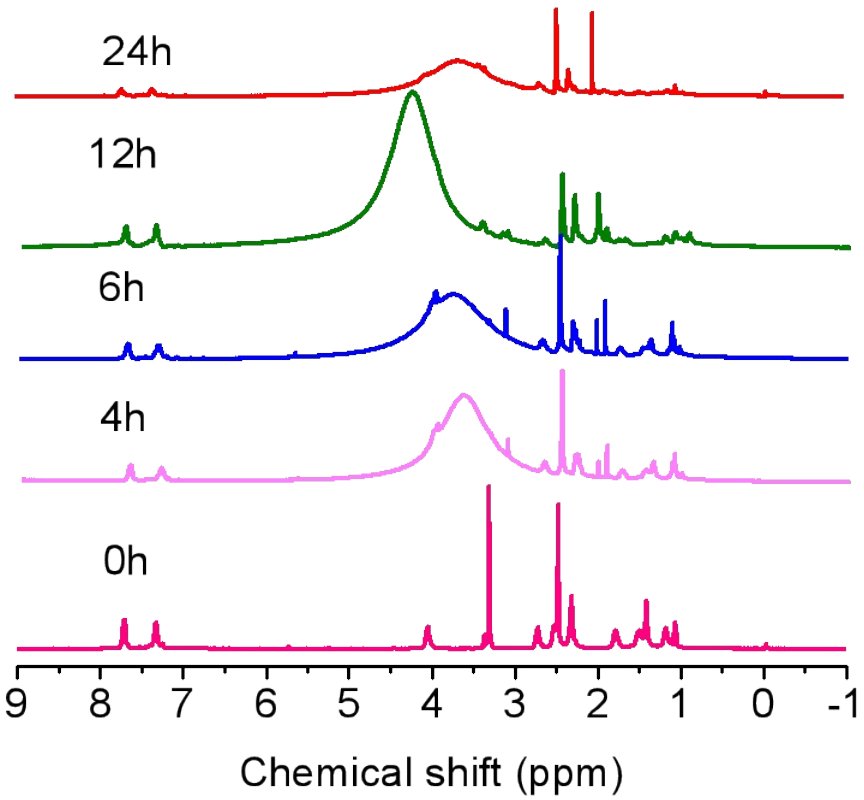


Figure S47. $^{1}H$ NMR spectra of P1 (P1a/2a/3a) following $H_2O_2$ treatment at different time intervals in *d*-DMSO.

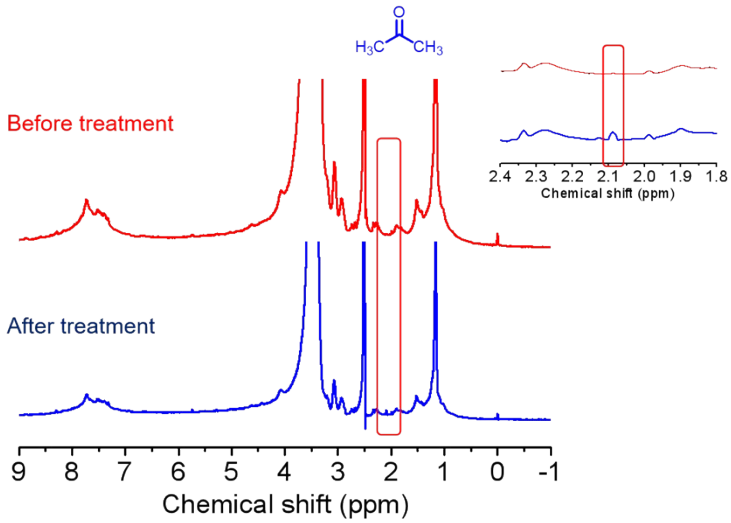


Figure S48. $^{1}$H NMR spectra of P7-TPP before and after light (650 nm) treatment in *d*-DMSO.

Table S1. The conjugation efficiency of TPP on the side chain of P7[a]

| TPP polymers | Feeding ratio of TPP (%) | Conjugation efficiency (%) |
|---|---|---|
| P7-TPP1 | 25 | 25 |
| P7-TPP2 | 50 | 50 |
| P7-TPP3 | 100 | 50 |

[a]Conditions: experiments carried out at 70 ℃ under nitrogen in THF. CuI = 0.04 M, $PdCl_2(PPh_3)_2$ = 0.02 M.